Dual-Hit: Glyphosate exposure at NOAEL level negatively impacts birth and glia-behavioural measures in heterozygous shank3 mutants

Sophie Sakkaki, Noemie Cresto, Raphaël Chancel, Maé Jaulmes, Emma Zub, Marine Blaquière, Pierre Sicard, Tangui Maurice, Sandrine Ellero-Simatos, Laurence Gamet-Payrastre, et al.

Dual-Hit: Glyphosate exposure at NOAEL level negativel impacts birth and glia-behavioural measures in heterozygous shank3 mutants

Sophie Sakkaki a,1, Noemie Cresto a,1, Rapha¨el Chancel a, Ma´e Jaulmes a, Emma Zub a, Marine Blaqui`ere a, Pierre Sicard b, Tangui Maurice c, Sandrine Ellero-Simatos d, Laurence Gamet-Payrastre d, Nicola Marchi a,1,*, Julie Perroy a,1,*

a *IGF, University of Montpellier, CNRS, INSERM, Montpellier, France*

b *PhyMedExp, INSERM, CNRS, CHU Montpellier, University of Montpellier, 34295 Montpellier, France*

c *MMDN, Univ Montpellier, EPHE, INSERM, Montpellier, France* d *Toxalim, INRAE, Toulouse, France*

Keywords:

NOAEL-Glyphosate Shank3 mutation Perinatal exposure Environmental contamination Genetic predisposition Neuroinflammation Neurodevelopmental disorders

---

Abbreviations:

ADHD, attention deficit hyperactivity disorder; ASD, Autism Spectrum Disorder; BBB, Blood Brain Barrier; CD31, Cluster of Differentiation 31 (Platelet endothelial cell adhesion molecule (PECAM-1); GBH, glyphosate-based herbicides; GFAP, Glial Fibrilary Acidic Protein; GLY, Glyphosate; IBA1, Ionized calcium Binfind Adapter protein 1; NMDA, N-Methyl-D-aspartic acid; NOAEL, Non-Observable Adverse Effect Level; NOR, Novel Object Recognition; PN21, Postnatal day 21; Shank, SH3 and multiple ankyrin repeat domains protein.

*** Corresponding authors at:**

Cerebrovascular and Glia Research, Institut de G´enomique Fonctionnelle (University of Montpellier, CNRS, INSERM), 141 rue de la Cardonille, 34094 Montpellier, Cedex 5, France (Nicola Marchi) Pathophysiology of synaptic transmission, Institut de G´enomique Fonctionnelle (University of Montpellier, CNRS, INSERM), 141 rue de la Cardonille, 34094 Montpellier, Cedex 5, France (Julie Perroy).

E-mail addresses:

nicola.marchi@igf.cnrs.fr (N. Marchi), julie.perroy@igf.cnrs.fr (J. Perroy).

1 These authors contributed equally.

A B S T R A C T

The omnipresence of environmental contaminants represents a health danger with ramifications for adverse neurological trajectories. Here, we tested the dual-hit hypothesis that continuous exposure to non-observable adverse effect level (NOAEL) glyphosate from pre-natal to adulthood represents a risk factor for neurological-associated adaptations when in the presence of the heterozygote or homozygote mutation of the Shank3 synaptic gene.

Ultrasound analysis of pregnant dams revealed patterns of pre-natal mortality with effects dependent on wild-type, Shank3$^{\Delta C}$/$^{+}$, or Shank3$^{\Delta C/\Delta C}$ genotypes exposed to NOAEL glyphosate (GLY) compared to unexposed conditions. The postnatal survival rate was negatively impacted, specifically in Shank3ΔC/+ exposed to GLY. Next, the resulting six groups of pups were tracked into adulthood and analyzed for signs of neuroinflammation and neurological adaptions. Sholl's analysis revealed cortical microgliosis across groups exposed to GLY, with Shank3$^{\Delta C/+}$ mice presenting the most significant modifications. Brain tissues were devoid of astrocytosis, except for the perivascular compartment in the cortex in response to GLY. Distinct behavioral adaptations accompanied these cellular modifications, as locomotion and social preference were decreased in Shank3$^{\Delta C/+}$ mice exposed to GLY. Notably, GLY exposure from weaning did not elicit glial or neurological adaptations across groups, indicating the importance of pre-natal contaminant exposure.

These results unveil the intersection between continuous pre-natal to adulthood environmental input and a pre-existing synaptic mutation. In an animal model, NOAEL GLY predominantly impacted Shank3$^{\Delta C/+}$ mice, compounding an otherwise mild phenotype compared to Shank3$^{\Delta C/\Delta C}$. The possible relevance of these findings to neurodevelopmental risk is critically discussed, along with avenues for future research.

--

1. Introduction

Neurodevelopmental disorders are characterized by behavioral and learning maladaptations, with increased incidence in past years. These disorders include autism spectrum disorder (ASD), attention deficit hyperactivity disorder (ADHD), and intellectual disability. As documented by the Centers for Disease Control and Prevention, the steady increase in the incidence of neurodevelopmental disorders these last decades (Baio et al., 2018; de la Paz & Canal-Bedia, 2021; Seretopoulos et al., 2020; Zeidan et al., 2022), cannot be explained only by changes in diagnostic criteria. Genetic and environmental factors can contribute to the development of neurodevelopmental disorders (Martin et al., 2018; Taylor et al., 2019). In this clinical framework, emerging evidence raises the possibility of potentially dangerous intersections between pre-existing neuronal mutations and continuous exposure to environmental contaminants (He et al., 2022; Shelton et al., 2012). However, studies examining this possibility are limited at the pre-clinical level.

Here, we tested the hypothesis that continuous dietary exposure to low-level glyphosate (GLY) introduces adverse phenotypes in the presence of a heterozygote SHANK3 gene mutation, the latter recognized in neurodevelopmental disorders. A set of genes at the synaptic level have been identified, whose monogenic mutation would generate ASD (B.M. et al., 2012; Bourgeron, 2015; Krumm et al., 2014; O ' Roak et al., 2012). SHANK3, a gene encoding a synaptic scaffolding protein involved in the formation, maturation, and plasticity of excitatory synapses (Boeckers et al., 2002; Sheng & Kim, 2000), displays mutations that trigger ASD in humans (Bonaglia et al., 2001; Durand et al., 2007; Phelan & McDermid, 2012; Sandin et al., 2017), and certain specific phenotypes in rodents (Delling & Boeckers, 2021; Kouser et al., 2013; Moutin et al., 2021; Sala et al., 2015). The fundamental premise that ASD is triggered by the interplay between genetic and environmental factors is reinforced by findings from pre-clinical studies. Contrary to humans, mice with heterozygous mutation of ASD-associated genes do not typically exhibit (or only minimally) ASD-like behavioral impairments in the aseptic and controlled environment of the laboratory (Jaramillo et al., 2017; Mei et al., 2016; Peça et al., 2011; Wang et al., 2016). By opposition, a homozygous mutation in mice does lead to such deficits. Thus, it is possible that introducing environmental stressors could expose phenotypes that are typically unrecognized in heterozygous animals.

This study focuses on GLY exposure as an environmental risk factor for adverse behavioral phenotypes (Cresto et al., 2023; Roberts et al., 2019; Von Ehrenstein et al., 2019). Acute toxicity of GLY appears to be very low on mammals with median lethal dose (DL50) ranging from 2000 mg/kg to 8000 mg/kg depending on species and studies and the official DL50 from US EPA (US environemental protection agency) is 5037 mg/kg. However, it has been shown that GLY exposure to lower dose can be toxic for the nervous, immune and reproductive

systems (Gandhi et al., 2021). Moreover, studies have demonstrated that diet is likely to be the major route of GLY exposure for the general population, especially in children (Fagan et al., 2020). Very few studies have examined the impact of dietary GLY exposure delivered chronically, fueling debates on its tangible effects on brain health (De Araujo et al., 2016; He et al., 2022; Lacroix & Kurrasch, 2023; Von Ehrenstein et al., 2019). From this background, we studied whether exposure to NOAEL GLY impacts phenotypes due to a mutation in the SHANK3 gene. We used wild-type, heterozygous or homozygous mice for SHANK3 gene deleted after exon 21 ($Shank3^{+/+}$, $Shank3^{\Delta C/+}$ and $Shank3^{\Delta C/\Delta C}$ (Kouser et al., 2013; Moutin et al., 2020)) and compared functional consequences of GLY daily administration, with two distinct protocols including pre-natal period or not, of Non Observable Adverse Effect Level (NOAEL; 50 mg/kg bw/day). We tested pregnancy and birth rates, biomarkers of brain inflammation, and behaviors. Our results illustrate how pre-natal to adulthood exposure to NOAEL GLY tilts the $Shank3^{\Delta C//+}$ mice phenotype, introducing extra-physiological adjustments. These results support the detrimental synergy between environmental and genetic predispositions or factors.

2. Material and methods

2.1. Animals

All animal procedures were conducted in accordance with the European Communities Council Directive, supervised by the IGF institute's local Animal Welfare Unit (A34-172–41) and approved by the French Ministry of Research (agreement numbers: APAFIS# 2,020,021,914,472,552 #24578 v4, APAFIS# 2020020610158031_v2, #17133–2018101615211943 v3). The Shank3ΔC mice have a deletion of exon 21 that includes the Homer-binding domain (Jackson Laboratory, Bar Harbor, ME) and were backcrossed to C57BL6/J mice.

2.2. Pellets production and dosage

Glyphosate (SigmaAldrich) was dissolved in a 9:1 volume/volume (v/v) mixture of methanol:acetone. The solution was dispersed over the vitamin powder (PV 200, Scientific Animal Food Engineering (SAFE, Augy, France)) and then homogenized in a rotavapor (Laborota 4000™; BUCHI Switzerland) for 30 min at 45 ◦C to evaporate the solvents and for 50 min at room temperature. Control feed was prepared as described above, with the vitamin powder incubated with a 9:1 mixture of methanol: acetone without GLY. The vitamin powder with or without GLY enrichment was sent to the Animal and Food Science Unit (SAAJ, Jouy en Josas, France) of the National Research Institute for Agriculture, Food and Environment (INRAE), which prepared control and GLY-enriched pellets from a mixture of our control or

GLY-enriched vitamin powders (1 %) with minerals complements (7 %) and other diet components (63 % carbohydrate, 5 % fat, 22 % protein, and 2 % cellulose). Eurofins (Nantes, France) quantified the GLY in the pellets using gas-chromatography–tandem mass spectrometry and liquid-chromatography–tandem mass spectrometry. The final concentrations were confirmed, and the control feed did not contain GLY.

2.3. Maternal NOAEL GLY exposure

Eight-week-old female and male C57BL/6J strains were bred and housed in the IExplore animal facility (Montpellier, France). Groups of Shank3$^{+/+}$, Shank3$^{\Delta C/+,}$ and Shank3$^{\Delta C/\Delta C}$ males (n = 36) and females (n = 72) were randomly housed regarding genotype five or six per cage, with a 12 h light/dark cycle, at a stable temperature of 21 ± 2 ◦C, and were allowed ad libitum access to food and water. For a five days mating period, the animals were divided into six groups (exposed and unexposed to GLY and by genotype: Shank3$^{+/+}$, Shank3$^{\Delta C/+}$, Shank3$^{\Delta C/\Delta C}$) and housed with one male and two females per cage (36 cages). During the mating period, the diet was switched to either the GLY-enriched or GLY-free (Fig. 1). Food and water consumption were monitored weekly during the mating and gestation period but not during the lactation period to avoid cannibalism. After the mating period, males were removed from the cages. Litters were changed at least once a week, and weaning was performed at PN21 for each litter to minimize the offspring's direct eating of pellet residues. The male offspring from exposed or non-exposed dams were separated, housed in 3 or 4 per cage according to their group, and fed accordingly. Weight, food, and water consumption were monitored.

2.4. Post-Weaning exposure

Heterozygous mice were bred, and all mice were grouped after weaning for genotype. For experiments, we used littermate males Shank3$^{+/+}$, Shank3$^{\Delta C/+}$, and Shank3$^{\Delta C/\Delta C}$. After weaning at PN21, each genotype was randomly divided into two groups: GLY exposed or unexposed. Weight, food, and water consumption were monitored weekly. The food pellets were weighed each week before and after resupplying for each cage. Food consumption was evaluated by subtracting these two measurements and dividing the result by the number of mice per cage. The same assessment was made for water consumption.

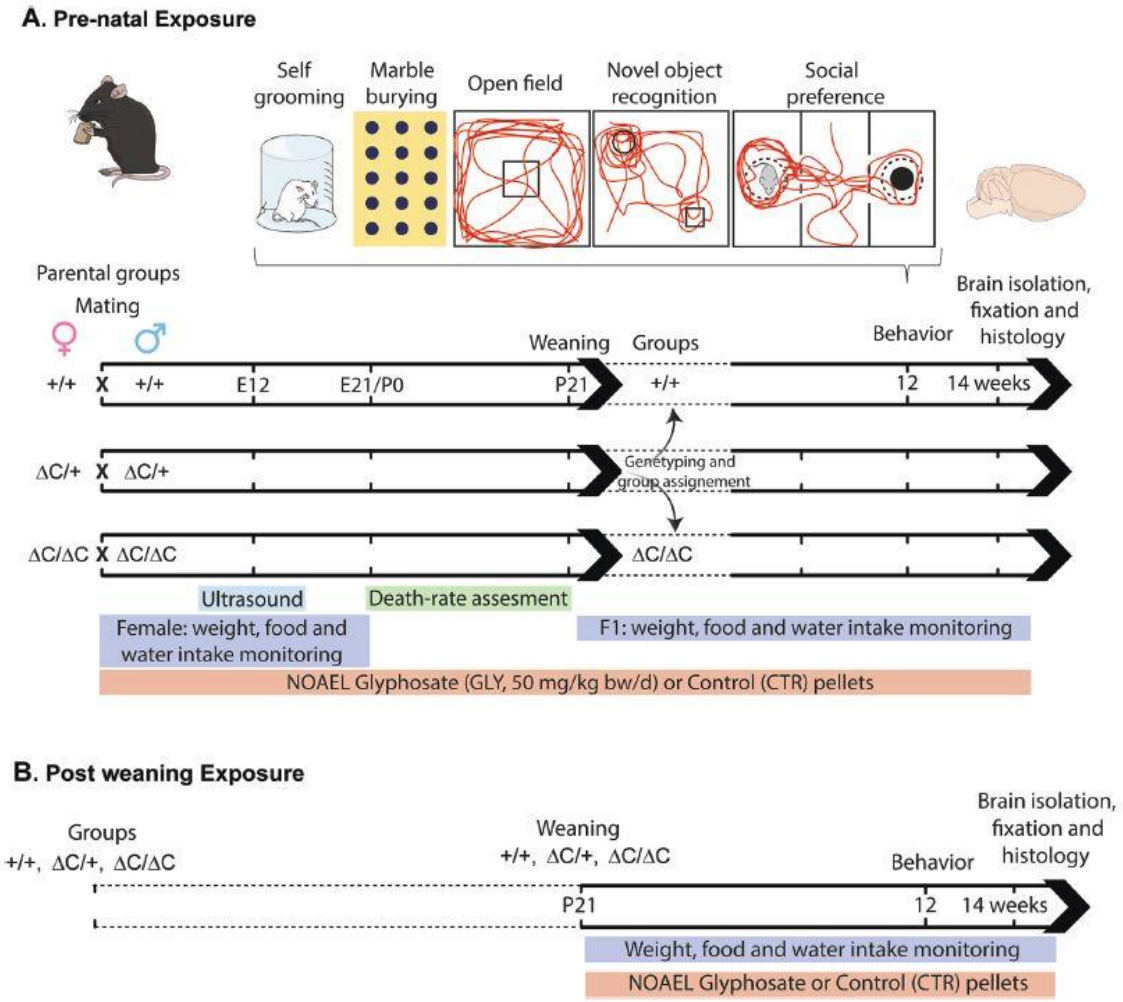

Fig. 1. Protocol overview. (A) To test the effects elicited from continuous exposure to GLY, from pre-natal to adulthood, and whether GLY exposure aggravates symptoms due to specific ASD-like synaptic mutations, WT (+/+), heterozygous Shank3 mice (ΔC/+) and homozygous Shank3 mice (ΔC/ΔC) were fed with a pellet containing European Non-Observable Adverse Effect Level (NOAEL) of GLY (50 mg/kg bw/d). The treatment was at mating, gestation, and lactation. Female weight, food, and water intake were monitored. An ultrasound was performed on pregnant mice at embryonic day 12 (E12). Mortality was assessed from birth to weaning. At weaning, animals were directly fed using pellets containing GLY. At 12 weeks, cognitive performances were evaluated using behavioral tasks: stereotyped and repetitive behaviors measuring self-grooming episodes and marble burying. Locomotion, anxiety, and memory using the open field apparatus, and social preference using the three chambers test. Videos were recorded and analyzed through automated video tracking systems (Noldus). At the end of the protocol (14 weeks), brains were collected and fixated to perform histology. **(B)** In parallel, another cohort of Shank3+/+, Shank3ΔC/+, and Shank3ΔC/ΔC mice was constituted; the GLY exposure started at the weaning until the end of the study. Weight, food, and water intake were monitored. At 12 weeks, cognitive performances were assessed using the tests previously described. At 14 weeks, brains were collected and fixated for histology.

2.5. Transcutaneous high-resolution ultrasound imaging during gestation

High-resolution ultrasound (Vevo 3100, Fujifilm/VisualSonics, Canada) was used to monitor the presence of live and dead embryos or fetuses in the same mothers. An MX550D ultrasound probe performed transcutaneous imaging of embryos and fetuses at 40 MHz. After anesthesia with 2.5 % of isoflurane and maintained at 2 % during the application of pre-warmed ultrasound gel, fetuses were examined, counted, and considered alive by the identification of a heartbeat.

2.6. Maternal behavioral experiments

After pups were weaned, two dams were kept in each cage, and nesting behavior related to motherhood and anxiety was assessed. *Nesting:* 6 g of nesting material was placed in home cages. Twenty-four hours later, the quantitative amount of nesting material that was actively pulled into the cage and the quality of the nest are assessed, and an experienced experimenter takes and analyzes photographs of the nests manually. *Postnatal mortality evaluation:* the mortality of the pups was monitored several times per day from the day of birth until one week, and then every day until weaning.

2.7. Behavioral tests

Behavioral experiments were performed on animals between 13 and 20 weeks old. Mice were housed in group cages with 4–3 individuals per cage, supplemented with enrichment cotton nests and nest boxes. Behavioral experiments were performed between 8:00 am – 4:00 pm in a light color wall room with control light devices. *Marble burying:* mice were placed individually in a clean cage with 10 cm thick bedding and 15 marbles evenly distributed on top of the bedding. After 30 min in the cage, the mice were removed. We evaluated the level of marble burying according to the following Score: 0 for a buried marble, 1 for a half-buried marble, and 2 for a visible marble. *Self-grooming*: mice were placed in a 25 cm Plexiglas cylinder and video monitored. Time spent self-grooming was visually measured during 10 min. *Open field and Novel object recognition task (NOR):* mice were tested in the open field apparatus (50 cm × 45 cm). The locomotor activity was recorded with the EthoVision XT video tracking system (Noldus, Wageningen, Netherlands). Animals were first habituated to the arena for 10 min. Each mouse was placed in the open field's periphery and allowed to freely explore the apparatus for 10 min, with the experimenter out of the animal's sight. The distance traveled and time spent in the central region were recorded by video tracking over the test session. The time spent in the center area is used as an anxiety index. One hour later, mice

were tested for object recognition in the same arena. They were submitted to a 10 min acquisition trial and placed in the arena with sample objects (A and A'). The animal's time to explore the samples (sniffing) was automatically recorded. A 10 min retention trial was performed one hour later. During this trial, one of the samples A, and another object, B were placed in the open field, and the times tA and tB the animal took to explore the two objects were recorded. A recognition ratio was defined as (tB / (tA + tB)). *Three Chambers Social preference test*: this test evaluates a mouse's preference for a congener compared to an object placed in an opposite compartment. Social behavior is altered in Shank3$^{\Delta C/\Delta C}$ mice (Kouser et al., 2013). The apparatus is a transparent cage with a central starting compartment and two side compartments where a circular grid cup (goal box) is placed at each extremity and where the congener and the object can be placed during testing. First, the mouse was placed in the central box and allowed to freely explore the apparatus for 10 min to attenuate its emotionality. One hour later, a C57Bl/6 congener from the same sex was placed in one goal box, and an object was placed in the opposite compartment. The mouse was then placed in the starting central compartment and allowed to explore the apparatus freely for 10 min. The position of the congener and object boxes was counterbalanced to avoid any potential spatial preference. The duration of exploration of each goal box (when the mouse is sniffing the grid delimiting the goal box) was automatically measured. The percentage of time the mouse took to explore the congener was used as an index of social preference. The social preference index is (time Congener / (time Object + time Congener)).

2.8. Histology and quantifications

Mice were deeply anesthetized with ketamine/xylazine and perfused intracardially with saline solution. The brains were carefully dissected and post-fixed overnight with PFA 4% at 4 ◦C. The next day, brains were cryoprotected overnight in phosphate buffer saline solution (PBS) containing 30 % sucrose. The brains were cut into 20 µm sections on a cryostat (Leica, Germany). Slices were stored in PBS with cryoprotectant at 20 ◦C until use. For immunofluorescence, slices were blocked with PBS-Horse serum-Triton (PBS with 20% of horse serum and 0.25% of Triton) for 1 h at room temperature, incubated overnight at 4 ◦C with primary antibodies in the blocking solution, washed three times with PBS, incubated 1 h30 with secondary antibodies in the blocking solution and washed three times with PBS before mounting with Fluoromount with DAPI (Invitrogen). Glial fibrillary acidic protein (chicken GFAP antibody, Abcam ab4674), ionized calcium-bound adaptor molecule 1 (rabbit IBA1 antibody, Wako 019–19741), and cluster of differentiation 31 (rat CD31 antibody, Abcam ab56299) antibodies were used to stain astrocytes, microglia and vessels border, respectively. *Sholl analysis*: Z-stack images were acquired at an epifluorescence microscope with a 40 X magnification (Apotome, Zeiss). Astrocytes were selected based on the GFAP staining, and microglia were selected based on the IBA1 staining. The ImageJ plugin 'Sholl analysis' (Ferreira et al., 2014) was used to measure the number of intersections between GFAP staining and the concentric circles spaced by 5 µm and centered on the astrocyte

nucleus. *Astrocytes vascular coverage:* The quantification of GFAP optical density around the microcapillary serves as a biomarker for assessing local astrocyte reactivity, which in turn is an indicator of inflammation in the vascular compartment (Kozberg et al., 2022). This measurement holds particular significance because glyphosate in the bloodstream due to continuous dietary ingestion may adversely affect microvessels at the blood–brain barrier, potentially leading to vascular wall damage and localized inflammation. Vessels were stained using CD31 antibody, and astrocytes were stained using GFAP antibody. Analysis was done on the parietal cortex. Using ImageJ, the mask of the CD31 staining was transferred to the GFAP channel, and the raw integrated density was measured around the mask.

2.9. Statistics

In utero and postnatal mortality rate data were analyzed using a Generalized Linear Model (GLM, SPSS software, IBM) to test the main effect of GLY exposure or genotype and the GLY exposure by genotype interaction effect. All other data are expressed as the mean ± SEM. Before statistical comparison, normality tests and variance analysis (Shapiro–Wilk test) were performed, and the appropriate two-sided parametric or nonparametric statistical test was used. For the parametric data set, statistical significance for within-group comparisons was determined by 2-way analysis of variance (ANOVA) followed by Bonferroni's post hoc test, while for the nonparametric data set, statistical significance was determined using Kruskal-Wallis followed by Dunn's post hoc test. For behavioral experiments (Novel object recognition and social preference test), red asterisks indicate differences related to the hypothetical value set at 0.5 using a one-sample *t*-test. Statistical analysis was performed using Prism 9.3.1 (Graphpad Software, CA, USA). Asterisk represents the difference between genotypes, while the hashtag symbol represents the GLY effect for each genotype. Statistics of pre-natal to adulthood exposure are reported in Table 1.

Table 1
Statistics table of pre-natal to adulthood exposure. For each groups and each measurment data mean, SEM, number of animals, normality test and ANOVA p-value were represented. Data highlighted in orange represent statistical significant results.

		Shank3 +/+ CTR		Shank3 +/+ GLY		Shank3ΔC/+ CTR		Shank3ΔC/+ GLY		Shank3 ΔC/ ΔC CTR		Shank3 ΔC/ ΔC GLY		P value
		Mean	SEM of discrepancy	Mean	SEM of discrepancy	Mean	SEM of discrepancy	Mean	SEM of discrepancy	Mean	SEM of discrepancy	Mean	SEM of discrepancy	
MORTALITY	**Womb dead fetuses per litter (%)**	**0 (N = 10)**	*0*	**7,205 (N = 10)**	*4.479*	**0 (N = 7)**	*0*	**3,333 (N = 8)**	*2.271*	**6,944 (N = 11)**	*3.049*	**5,641 (N = 14)**	*2.243*	
Fig. 2	*Shapiro-Wilk normality test*	*invalid mean = 0*		*no*		*invalid mean = 0*		*no*		*no*		*no*		
	Generalised Linear Model													*<0,01; ******
	Post-natal mortality rate per litter (%)	**31,60 (N = 14)**		**37,50 (N = 12)**		**36,77 (N = 17)**		**63,52 (N = 16)**		**41,18 (N = 12)**		**38,56 (N = 15)**		
	Shapiro-Wilk normality test	*no*		*no*		*no*		*no*		*yes*		*no*		
	Generalised Linear Model													***0.048***
	Dams weight gain (%)													
	Shapiro-Wilk normality test	*yes*		*yes*		*yes*		*yes*		*yes*		*yes*		
	Two-way ANOVA (group effect)													*0.1356*
	Dams food intake (g/ kg bw/d)													
	Shapiro-Wilk normality test	*yes*		*yes*		*yes*		*yes*		*yes*		*yes*		
	Two-way ANOVA (group effect)													***0,0001; ******
	Dams water intake (g/ kg bw/d)													
	Shapiro-Wilk normality test	*yes*		*yes*		*yes*		*yes*		*yes*		*yes*		
	Two-way ANOVA (group effect)													*0.2371*
	Nesting													
	Shapiro-Wilk normality test	*no*		*no*		*no*		*no*		*yes*		*no*		
	Kruskal-Wallis test													*0.1469*
	Theoretical glyphosate exposure													
	Shapiro-Wilk normality test	*yes*		*yes*		*yes*		*yes*		*yes*		*yes*		
	Two-way ANOVA (group effect)													***0.0024***
PHYSIO	**Weight gain (%)**													
PARAMETERS														
Fig. 3	*Shapiro-Wilk normality test*	*yes*		*yes*		*yes*		*yes*		*yes*		*yes*		
	Two-way ANOVA (group effect)													*<0,0001; *******
														(continued on next page)
	Food intake (g/ kg bw/ d)													
	Shapiro-Wilk normality test	*yes*		*yes*		*yes*		*yes*		*yes*		*yes*		
	Two-way ANOVA (group effect)													*0.1596*
	Water intake (g/ kg bw/ d)													
	Shapiro-Wilk normality test	*yes*		*yes*		*yes*		*yes*		*yes*		*yes*		
	Two-way ANOVA (group effect)													*0.6438*
	Theoretical glyphosate exposure													
	Shapiro-Wilk normality test	*yes*		*yes*		*yes*		*yes*		*yes*		*yes*		
	Two-way ANOVA (group effect)													*0,024; **
HISTOLOGY	**Microglia sholl parietal cortex**													
Fig. 4	*Shapiro-Wilk normality test*	*yes*		*yes*		*yes*		*yes*		*yes*		*yes*		
	Two-way ANOVA (group effect) "+/+ CTR Vs +/+ GLY"													*<0,0001; ******
	Two-way ANOVA (group effect) "ΔC/ + CTR Vs ΔC/+ GLY"													*<0,0001; ******
	Two-way ANOVA (group effect) "ΔC/ ΔC CTR Vs ΔC/ΔC GLY"													*<0,0001; ******
	Microglia sholl hippocampus													
	Shapiro-Wilk normality test	*yes*		*yes*		*yes*		*yes*		*yes*		*yes*		
	Two-way ANOVA (group effect) "+/+ CTR Vs +/+ GLY"													*<0,0001; ******
	Two-way ANOVA (group effect) "ΔC/ + CTR Vs ΔC/+ GLY"													*0.172*
	Two-way ANOVA (group effect) "ΔC/ ΔC CTR Vs ΔC/ΔC GLY"													*0.2158*
	Microglia number of intersection parietal cortex (5–30 µm)	**6,792 (N = 4, n = 40)**	*0.2555*	**4,372 (N = 3, n = 30)**	*0.1967*	**7,846 (N = 4, n = 40)**	*0.2682*	**3,728 (N = 3, n = 30)**	*0.1839*	**6,115 (N = 4, n = 40)**	*0.2469*	**4,158 (N = 3, n = 20)**	*0.2816*	
	Shapiro-Wilk normality test	*yes*		*yes*		*yes*		*yes*		*yes*		*yes*		
	Ordinary one-way ANOVA													*<0,0001; ******

	Microglia number of intersection parietal cortex (35–60 µm)	2,167 (N = 4, n = 40)	*0.4515*	0,2333 (N = 3, n = 30)	*0.06521*	2,721 (N = 4, n = 40)	*0.3553*	0,2778 (N = 3, n = 30)	*0.08162*	2,506 (N = 4, n = 40)	*0.5102*	0,1503 (N = 3, n = 20)	*0.05197*	
	Shapiro-Wilk normality test	*no*		*no*		*no*		*no*		*no*		*no*		
	Kruskal-Wallis test													***<0,0001;*** ****
	Microglia number of intersection hippocampus (5–30 µm)	7,328 (N = 4, n = 31)	*0.2653*	8,625 (N = 3, n = 24)	*0.2375*	7,618 (N = 4, n = 32)	*0.2334*	8,09 (N = 3, n = 24)	*0.2097*	7,474 (N = 4, n = 32)	*0.229*	7,667 (N = 3, n = 24)	*0.3058*	
	Shapiro-Wilk normality test	*yes*		*yes*		*yes*		*yes*		*yes*		*yes*		
	Ordinary one-way ANOVA													***0,0040;*** **
	Microglia number of intersection parietal cortex (5–30 µm) normalization			64,36 (n = 30)	*2.096*			47,51 (n = 30)	*2.344*			60,03 (n = 20)	*4.607*	
	Shapiro-Wilk normality test			*yes*				*yes*				*yes*		
	Ordinary one-way ANOVA													***<0,0001;*** ****
	Microglia number of intersection parietal cortex (35–60 µm) normalization			10,77 (n = 30)	*3.01*			10,21 (n = 30)	*3*			6,312 (n = 20)	*2.072*	
	Shapiro-Wilk normality test			*no*				*no*				*no*		
	Kruskal-Wallis test													*0.8117*
	Microglia number of intersection hippocampus (5–30 µm) normalisation			105,7 (n = 24)	*7.171*			103,7 (n = 24)	*2.688*			101,7 (n = 24)	*4.057*	
	Shapiro-Wilk normality test			*no*				*yes*				*yes*		
	Kruskal-Wallis test													*0.0923*
Fig. 5	**Astrocyte RID parietal cortex (AU)**	15,588,064 (N = 4)	*3,081,642*	14,292,500 (N = 4)	*1,130,348*	22,383,156 (N = 4)	*5,859,558*	37,085,684 (N = 4)	*8,405,432*	20,444,732 (N = 4)	*5,190,114*	56,565,767 (N = 3)	*10,707,914*	
	Shapiro-Wilk normality test	*yes*		*yes*		*yes*		*yes*		*yes*		*yes*		
	Ordinary one-way ANOVA													***0,0018;*** **
	Astrocyte RID parietal cortex normalization			91,68 (N = 4)	*7.251*			166,1 (N = 4)	*37.64*			276,7 (N = 3)	*52.37*	
	Shapiro-Wilk normality test			*yes*				*yes*				*yes*		
	Ordinary one-way ANOVA													0,0182; *
	Astrocyte RID hippocampus (AU)	102,453,914 (N = 4)	*18,097,074*	66,343,706 (N = 4)	*8,821,028*	110,955,275 (N = 4)	*32,540,156*	66,979,657 (N = 4)	*15,965,783*	119,626,504 (N = 4)	*4,386,149*	91,618,157 (N = 4)	*7,473,059*	
	Shapiro-Wilk normality test	*yes*		*yes*		*yes*		*yes*		*yes*		*yes*		
	Ordinary one-way ANOVA													*0.7769*
	Astrocyte RID hippocampus normalization			84.28	*8.61*			78.39	*14.41*			76.46	*6.237*	
	Shapiro-Wilk normality test			*yes*				*yes*				*yes*		
	Ordinary one-way ANOVA													*0.8765*
	Astrocyte sholl hippocampus													
	Shapiro-Wilk normality test	*yes*		*yes*		*yes*		*yes*		*yes*		*yes*		
	Two-way ANOVA (group effect) "+/+ CTR Vs +/+ GLY"													*<0,0001;* ****
	Two-way ANOVA (group effect) "ΔC/+ CTR Vs ΔC/+ GLY"													*0.4471*
	Two-way ANOVA (group effect) "ΔC/ΔC CTR Vs ΔC/ΔC GLY"													***0,0266;*** *
BEHAVIOR	**Marble score**	13 ((N = 14)	*1.038*	13,67 (N = 12)	*1.384*	17,8 (N = 10)	*0.9919*	14,8 (N = 10)	*1.02*	21,18 (N = 17)	*0.8235*	22,73 (N = 11)	*0.5092*	
Fig. 6	*Shapiro-Wilk normality test*	*yes*		*yes*		*yes*		*yes*		*yes*		*yes*		
	Ordinary one-way ANOVA													***<0,0001;*** ****
	Marble score normalization			106,3 (N = 12)	*9.677*			93,15 (N = 10)	*5.729*			107,3 (N = 11)	*2.782*	
	Shapiro-Wilk normality test			*yes*				*yes*				*yes*		
	Ordinary one-way ANOVA													***0,03;*** *
	Grooming time (s)	79,69 (N = 12)	*8.799*	71,33 (N = 11)	*8.56*	65,74 (N = 11)	*11.04*	67,43 (N = 9)	*9.607*	131,4 (N = 16)	*12.29*	145,7 (N = 11)	*20.29*	
	Shapiro-Wilk normality test	*yes*		*yes*		*yes*		*yes*		*yes*		*yes*		
	Ordinary one-way ANOVA													***<0,0001;*** ****
	Open field distance (cm)	3433 (N = 22)	*134.5*	4060 (N = 10)	*272.7*	3654 (N = 11)	*238.2*	2504 (N = 7)	*284.7*	2957 (N = 17)	*158*	3287 (N = 10)	*297.5*	
	Shapiro-Wilk normality test	*yes*		*yes*		*no*		*no*		*yes*		*yes*		
	Kruskal-Wallis test													*0.219*
	Open field distance normalization													
	Shapiro-Wilk normality test			*yes*				*no*				*yes*		
	Kruskal-Wallis test													***0,005;*** **
	Open field time in center	24,85 (N = 10)	*6.451*	23,34 (N = 10)	*5.125*	21,58 (N = 11)	*4.026*	16,62 (N = 7)	*5.237*	29,87 (N = 17)	*8.941*	30,78 (N = 10)	*7.075*	

Shapiro-Wilk normality test	*yes*		*yes*		*no*		*yes*		*no*		*yes*	
Kruskal-Wallis test												*0.614*
NOR discrimination ratio	**0,7098 (N = 22)**	*0.02917*	**0,7721 (N = 10)**	*0.04689*	**0,6784 (N = 11)**	*0.05079*	**0,7254 (N = 7)**	*0.05584*	**0,6157 (N = 17)**	*0.05576*	**0,4945 (N = 10)**	*0.04726*
Shapiro-Wilk normality test	*yes*		*yes*		*yes*		*yes*		*yes*		*yes*	
P value summary, One sample t test (hypothetical mean: 0.5)	****		***		**		**		*ns*		*ns*	
Ordinary one-way ANOVA												*0,0011; **
NOR normalization			**108,6 (N = 10)**	*6.606*			**107,7 (N = 7)**	*8.293*			**80,32 (N = 10)**	*7.676*
Shapiro-Wilk normality test			*yes*				*yes*				*yes*	
Ordinary one-way ANOVA												*0,0201; *
Social preference (median)	**0,6441 (N = 10)**		**0,4801 (N = 10)**		**0,5619 (N = 10)**		**0,4949 (N = 8)**		**0,6687 (N = 8)**		**0,634 (N = 10)**	
Shapiro-Wilk normality test	*yes*		*yes*		*yes*		*yes*		*yes*		*no*	
Wilcoxon signed rank test (hypothetical median: 0.5)	**		*ns*		**		*ns*		**		*	
Ordinary one-way ANOVA												*<0,0001; ****
Social preference normalisation			**67,46 (N = 10)**	*6.361*			**80,13 (N = 8)**	*6.696*			**94,11 (N = 10)**	*5.127*
Shapiro-Wilk normality test			*yes*				*yes*				*no*	
Kruskal-Wallis test												*0,0123; *

Fig. 2. Perinatal GLY exposure induces in utero death and increases postnatal mortality in Shank3$^{\Delta C/þ}$. (A-D) An ultrasound was performed on anesthetized pregnant mice at embryonic day 12 (E12) (+/- 1 day) for all genotypes. The number of fetuses was counted for each pregnant mouse, and based on the heartbeat coupled with Doppler imaging, the number of dead fetuses was obtained. +/+ CTR, N = 10; +/+ GLY, N = 10; ΔC/+ CTR, N = 7; ΔC/+ GLY, N = 8; ΔC/ΔC CTR, N= 11; ΔC/ΔC GLY, N = 14. Generalized Linear Model (p interaction genotype X GLY < 0.01) (E) After birth, mortality of the pups was monitored several times per day from the day of birth until one week and then every day until weaning. +/+ CTR, N = 14; +/+ GLY, N = 12; ΔC/+ CTR, N = 17; ΔC/+ GLY, N = 16; ΔC/ΔC CTR, N = 12; ΔC/ΔC GLY, N = 15.Generalized Linear Model (p interaction genotype X GLY = 0.043). (F-H) Dams' weight gain (in percentage), food, and water intake (g/kg bw/d) were monitored during the three weeks of pregnancy to ensure good nutrition and global health. +/+ CTR, N = 12; +/+ GLY, N = 8; ΔC/+ CTR, N = 9; ΔC/+ GLY, N = 8; ΔC/ΔC CTR, N = 12; ΔC/ΔC GLY, N = 14. E, 2-way ANOVA (p = 0.1356), F, 2-way ANOVA (p < 0.001), G, 2-way ANOVA (p = 0.2371). (I) GLY exposure was assessed by quantifying it in the feed pellets and monitoring the daily food consumption of mice. (J-K) Dams' nesting capabilities were assessed. +/+ CTR, N = 7; +/+ GLY, N = 5; ΔC/+ CTR, N = 6; ΔC/+ GLY, N = 7; ΔC/ΔC CTR, N = 7; ΔC/ΔC GLY, N = 7. Kruskal-Wallis test (p = 0.1469). Asterisks indicate statistical significance (* p < 0.05; ** p < 0.01; *** p < 0.001; **** p < 0.0001), ns: non-significant.

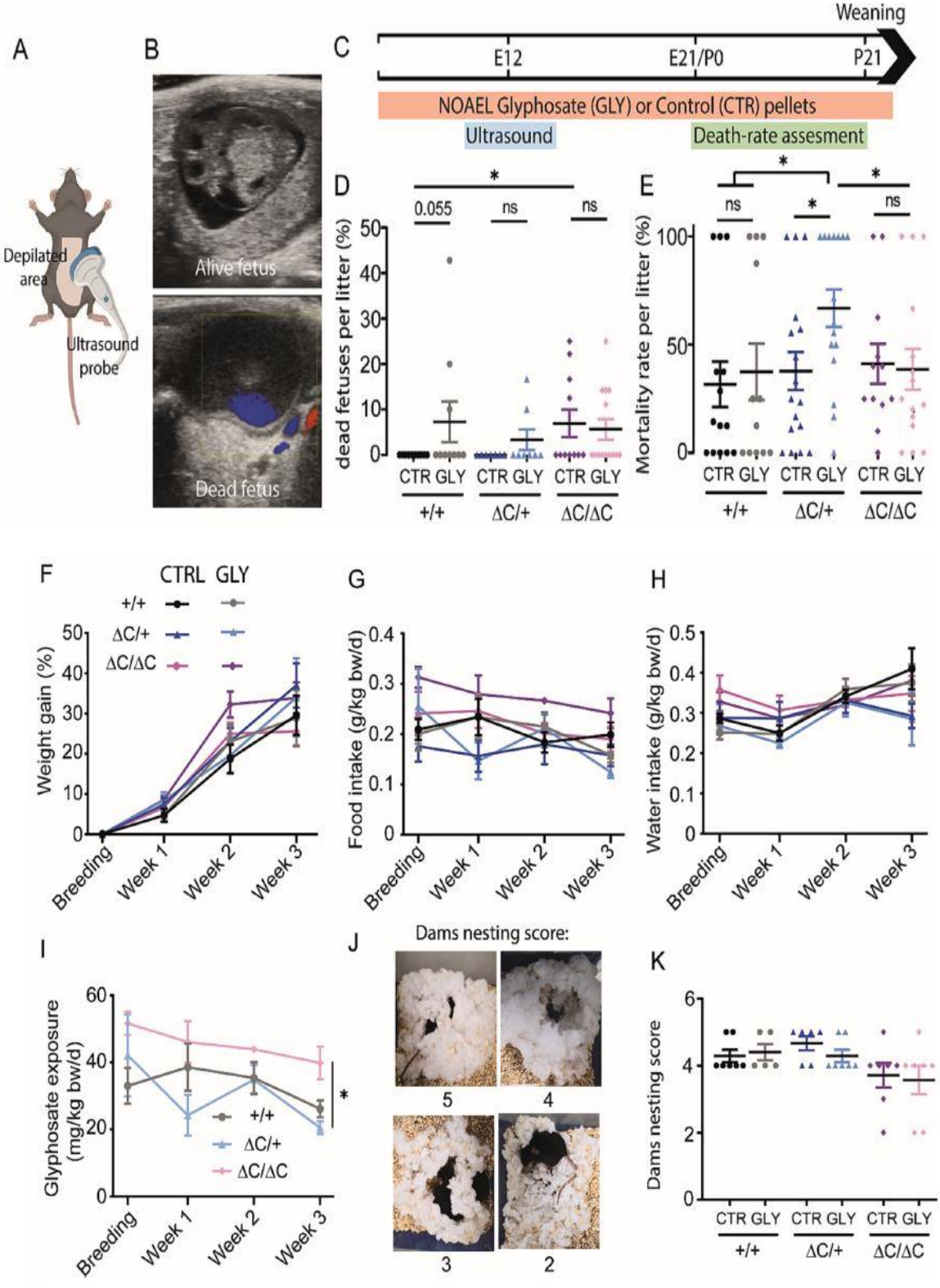
A
B
C
Weaning
E12
E21/P0
P21
NOAEL Glyphosate (GLY) or Control (CTR) pellets
Ultrasound
Death-rate assesment
Depilated area
Ultrasound probe
Alive fetus
Dead fetus
D
dead fetuses per litter (%)
0.055
ns
ns
CTR GLY CTR GLY CTR GLY
+/+ ΔC/+ ΔC/ΔC
E
Mortality rate per litter (%)
ns
ns
CTR GLY CTR GLY CTR GLY
+/+ ΔC/+ ΔC/ΔC
F
CTRL GLY
+/+
ΔC/+
ΔC/ΔC
Weight gain (%)
Breeding
Week 1
Week 2
Week 3
G
Food intake (g/kg bw/d)
H
Water intake (g/kg bw/d)
I
Glyphosate exposure (mg/kg bw/d)
J
Dams nesting score:
5
4
3
2
K
Dams nesting score
CTR GLY CTR GLY CTR GLY
+/+ ΔC/+ ΔC/ΔC

Fig. 3. F1 weight gain, food, and water intakes monitoring. (A) F1 weight gain (grams (g)), food (B), and water intakes (C) expressed as g or ml/g of body weight (gBW) / day(d) were monitored from weaning to 7 weeks. (D) Theoretical GLY exposure of F1 was evaluated based on food consumption and Eurofin's GLY concentration measurment. Body weight:: +/+ CTR, N = 19; +/+ GLY, N = 16; ΔC/+ CTR, N = 16; ΔC/+ GLY, N = 8; ΔC/ΔC CTR, N = 5; ΔC/ΔC GLY, N = 6. Food and water intakes (N = cages): +/+ CTR, N = 4; +/+ GLY, N = 4; ΔC/+ CTR, N = 5; ΔC/+ GLY, N = 2; ΔC/ΔC CTR, N = 2; ΔC/ΔC GLY, N = 2 s. Glyphosat theoretical exposure (N = cages): +/+ GLY, N = 4; ΔC/+ GLY, N = 2; ΔC/ΔC GLY, N = 2. A, 2-way ANOVA ($p < 0.001$), B, 2-way ANOVA ($p = 0.1598$), C, 2-way ANOVA ($p = 0.6438$). D, 2-way ANOVA ($p = 0.0240$).

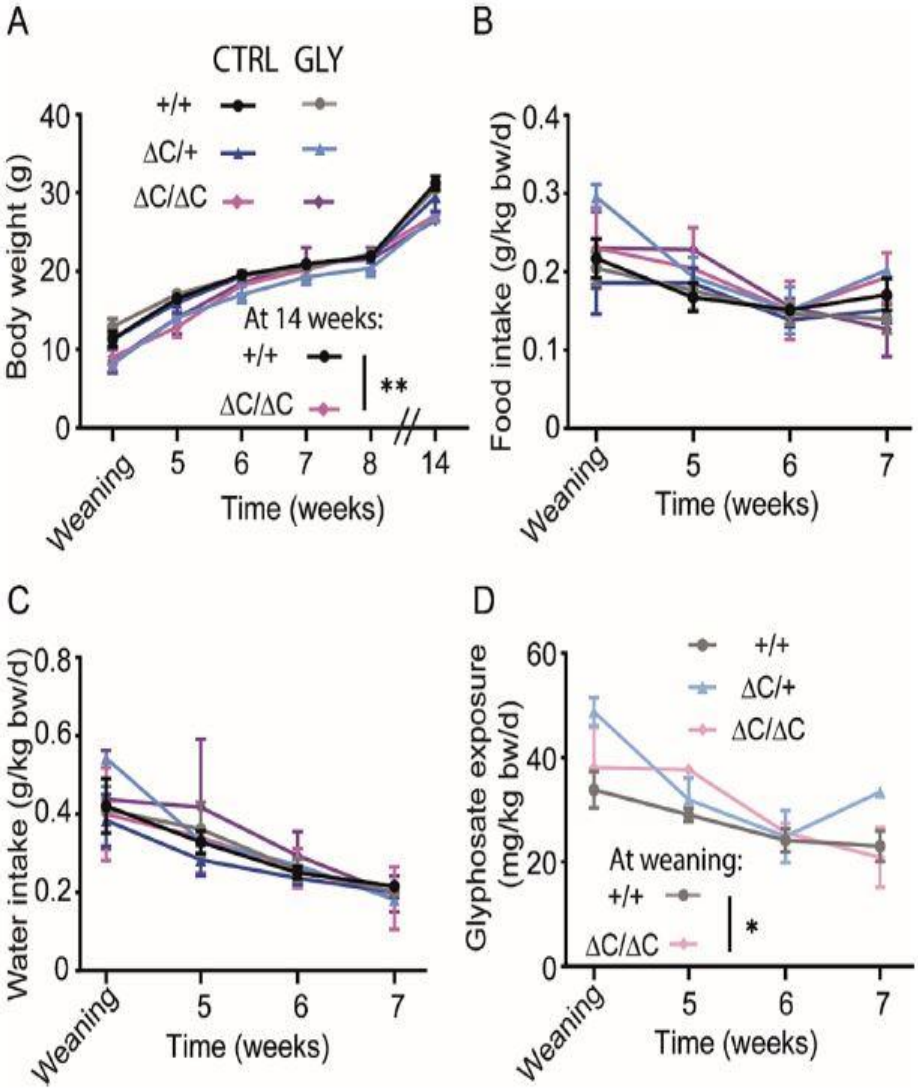

3. Results

3.1. Pre- and postnatal viability and weight gain trajectories: Interaction between genotype and GLY exposure

Fig. 1 illustrates the experimental design. We first examined whether exposure to dietary NOAEL GLY starting prenatally impacts pregnancies in Shank3ΔC/ΔC, Shank3ΔC/+, and wild-type, Shank3+/+ dams (Fig. 1A). Using ultrasound monitoring at embryonic day 12 (E12), we found a statistically significant interaction effect of GLY exposure and genotype on the mortality rate of fetuses in utero and those alive. GLY exposure was associated with an increase in the number of not viable fetuses in the womb in Shank3$^{\Delta C/+}$ and Shank3$^{+/+}$ mice (Fig. 2A - D). In Shank3$^{\Delta C/\Delta C}$ mice, the number of dead fetuses in the womb and the postnatal mortality rate are higher than in Shank3$^{\Delta C/+}$ and Shank3$^{+/+}$ mice, with no additional effect of GLY exposure. Postnatal mortality specifically increased in GLY-exposed Shank3$^{\Delta C/+}$ (Fig. 2E), unveiling a possible composite impact in these experimental conditions. Interestingly, we did not find any differences in weight gain (Fig. 2, F), food and water intakes (Fig. 2, G, H), and maternal behavior (Fig. 2, J-K) across genotypes and GLY groups, all factors that could have influenced pups' survival. Using measured concentration of GLY in pellets and the mother's food intake, we calculated the theoretical GLY exposure during pregnancy (L. Smith et al., 2020). All mice were similarly exposed to GLY (Fig. 2, I). Next, we tracked the offspring from weaning into adulthood. All animals across groups showed similar weight gain trajectories, with similar food and water intakes (Fig. 3A-C). Mice across genotypes were exposed to GLY similarly (Fig. 3D).

3.2. Cellular signs of neuroinflammation in adults depend on GLY exposure schedule and genotype

From this set of results, we explored the neuroinflammatory and neurological-associated adaptations emerging in adulthood from NOAEL GLY exposure and Shank3ΔC mutations. Glial cells are critical in brain disease conditions (Vargas et al., 2005). Importantly, in mice, GLY ingestion triggers pro-inflammatory cytokines production in the brain (Winstone et al., 2022), although evidence refers to exposure levels higher than the NOAEL dose. Here, we measured morphological alterations of microglia and astrocytes associated with continuous GLY exposure from pre-natal stages and compared it to post-weaning exposure only, in adulthood. First, we examined microglia in the parietal cortex and hippocampus using Sholl analysis to characterize changes in the process arbor based on the IBA1 staining (Fig. 4, A).

NOAEL GLY exposure elicited microglial modifications in the parietal cortex in all three genotypes: Shank3$^{+/+}$, Shank3$^{\Delta C/+}$, and Shank3$^{\Delta C/\Delta C}$ mice (Fig. 4, B1 - B3), while the hippocampus was spared (Fig. 4, C1 - C3, F, I). In the cortex, we report a morphological indication of microglia activation, in particular shorter cellular processes extending from the soma in all genotypes exposed to GLY, with an activation pattern quantifiable at 5–30 μm and 35–60 μm distance from the soma (Fig. 4, D, E, G, H). Notably, the effect of GLY exposure on microglial cells was more pronounced in Shank3$^{\Delta C/+}$ than in WT groups (Fig. 4, G), suggesting a possible genetic susceptibility. In the parietal cortex of Shank3$^{\Delta C/\Delta C}$, the microglial process arbor shows fewer ramifications than the two other genotypes in the control non-exposed condition, highlighting a genetic susceptibility given by the Shank3$^{\Delta C}$ mutation for microglial activation. Next, we tested whether microglial modifications exist if NOAEL GLY dietary exposure starts from PN21, avoiding perinatal stages. Supplemental Fig. 1 only shows marginal changes in IBA1 immunoreactivity in GLY-exposed conditions compared to control (CTR). These data suggest that GLY presence during perinatal development could be critical to trigger a microglial pathological imprint. To further elucidate this phenomenon, additional investigations could examine the complex alterations in molecular pathways associated with inflammatory responses. Next, we evaluated astrocytes' immunoreactivity (Fig. 5). Astrocytes switch in response to central nervous system pathologies from a resting to a reactive state by changing their morphology. This process is characterized by the upregulation of glial GFAP with hypertrophy. In the parietal cortex (Fig. 5, A), NOAEL GLY exposure induced accumulation of GFAP around vessels in Shank3$^{\Delta C/+}$ and Shank3$^{\Delta C/\Delta C}$ mice compared to their non-exposed control (Fig. 5, D-G), indicating perivascular activations (Fig. 5, B, E, H). In the hippocampus, astrocytes in Shank3$^{+/+}$ mice exposed to GLY displayed minimal or no adjustments (Fig. 5, C, F1 - F3). Next, we tested the effects of post-weaning exposure to GLY from PN21. We found no differences in astrocyte morphology in Shank3$^{+/+}$ and Shank3$^{\Delta C/+}$ genotypes for both brain structures (Supplemental Fig. 2).

3.3. Behavioral adaptations depend on Shank3$^{\Delta C}$ mutation and GLY exposure

Evidence links glial cell activations with specific behavioral adaptations and adverse neurological trajectories (Allen & Eroglu, 2017; Liddelow et al., 2017; Vargas et al., 2005). Here we performed behavioral phenotyping using translational relevant tests to neurodevelopmental conditions, focusing on autism–like phenotype considering the role of Shank3ΔC mutation in this disease (Kouser et al., 2013; Moutin et al., 2020). In the marble-burying test, unexposed Shank3$^{\Delta C/+}$ and Shank3$^{\Delta C/\Delta C}$ mice buried significantly fewer objects than the Shank3$^{+/+}$ (Fig. 6, A - C). This result was expected as mice carrying Shank3 mutations show an aversion to novelty (Kouser et al., 2013; Peça et al., 2011). Next, we evaluated the time mice spent self-grooming. Excessive self-grooming is considered both a manifestation of anxiety and obsessive–compulsive-like behavior. Shank3$^{\Delta C/\Delta C}$ mice spend increased time self-grooming (Fig. 6, D) (Kouser et al., 2013; Moutin et al., 2021). However,

we found no difference between Shank3$^{+/+}$ and Shank3$^{\Delta C/+}$ genotypes and no additional effect of GLY exposure. We performed the open field test to measure the natural locomotion and explorative behavior in an enclosed arena (Fig. 6, E). We first evaluated locomotion and found that GLY exposure significantly reduced the distance traveled in the Shank3$^{\Delta C/+}$ group (Fig. 6, G, H). Shank3$^{\Delta C/+}$ and Shank3$^{+/+}$ mice spent comparable time in the center zone, excluding anxiety-like traits. NOAEL GLY exposure did not impact this behavior (Fig. 6, I). To assess working memory, mice were tested for novel object recognition (NOR; Fig. 6, F). If the discrimination ratio is under 0.5, the mice explore the familiar object preferentially (Fig. 6, J, K). We found no difference between Shank3$^{\Delta C/+}$ and Shank3$^{+/+}$ genotypes and their respective GLY exposure conditions, all these mice explore more the new object (Fig. 6, J, K). Conversely, Shank3ΔC/ΔC mice have a discrimination ratio no different than 0.5 and GLY exposure does not affect this outcome.

To complete this behavioral phenotyping, we assessed social preference in a three-chamber test (Fig. 6, L). Exposure to GLY induces a deficit in social preference in Shank3$^{+/+}$ and Shank3$^{\Delta C/+}$ mice, as the mean ratio of exposed mice is not different from 0.5 (Fig. 6, M, N). Finally, we tested the effects of post-weaning NOAEL GLY exposure on behavior. We found no impact of GLY exposure in the self-grooming time (Figure supp 3, D), in the time spent in the center of the open field (Figure supp 3, E, I), in locomotion (Figure supp 3, G, H), in the NOR test (Figure supp 3, J, K), and in the three-chamber social preference test (Figure supp 3, L-N). The only difference found was an increase in the marble score of the Shank3$^{+/+}$ GLY group, reaching approximately the Shank3ΔC/+ level (Figure supp 3, C). Maternal exposure to GLY appears influential in shaping long-term behavioral adaptations.

4. Discussion

Understanding the impact of environmental contaminant exposure on brain health and function is a fundamental public health concern, particularly if genetic risk factors pre-exist. While studies have reported adverse effects of GLY on health, it is essential to consider that the levels of GLY used in varying studies are often higher than what is found in food and water (Costas-Ferreira et al., 2022). In this pre-clinical work, we designed a protocol to understand the impact of continuous dietary NOAEL GLY intake on brain function in the presence of SHANK3 mutations, the latter predisposing to neurodevelopmental disorders in humans. Our data outline a double-hit setting where an environmental input and a pre-existing synaptic Shank3ΔC/+ mutation can synergistically and negatively impact specific birth and neurological-associated trajectories. Overall, a significant impact of a GLY-containing diet is reported on pups' viability, the emergence of glial morphological adaptations, and atypical adult social behaviors, with a specific impact on mice carrying a heterozygous mutation of the SHANK3 gene. A predominant effect of homozygous mutation triggers phenotypic

adaptations, which are not worsened by the selected protocol. The presented work is consistent with previous studies showing how genetic variations can influence the brain's response to environmental poisoning and increase susceptibility to specific neurological conditions (Boyd et al., 2022; Miguel et al., 2023). NOAEL GLY exposure during pregnancy significantly increased the mortality rate per liter of Shank3ΔC/+ dams. Consistently, some studies have examined the association between ASD and fetal abnormalities (Ploeger et al., 2010; Regev et al., 2022). Maternal autism is also associated with preterm birth, but likely due to an increased frequency of medically indicated preterm births (Sundelin et al., 2018). Hence, embryos from mothers with ASD or siblings of individuals with ASD may have lower viability rates than embryos from healthy groups. While these studies suggest potential associations between ASD and the viability of embryos or pups at birth, the observed differences are generally small and do not imply causation. *4.1. Genetic predisposition and environmental input: The emergence of neurological-associated adaptations* Our results show that pre-natal NOAEL GLY exposure leads explicitly to the disappearance of social preference in $Shank3^{+/+}$ and $Shank3^{\Delta C/+}$ mice. This is one major characteristic of the ASD mice model as it mimics social impairments in patients with ASD. $Shank3^{\Delta C/\Delta C}$ exposed and non-exposed have a ratio above 0.5, which could surprisingly suggest a typical social preference. However, we must remember their natural avoidance of objects that complexify the interpretation and could mask their social phenotype. The hippocampal neuronal circuits are responsible for feeling and consolidating emotions, learning, and memory. The impact of GLY on the synaptic plasticity in hippocampal circuits has been widely studied (see canonical studies, referring primarily to Roundup (Cattani et al., 2014, 2021)). Likewise, subchronic and chronic exposures of mice to oral glyphosate-based herbicides (GBH) administration decreased exploratory activity. It increased anxiety and depression-like behaviors in rodents, which was associated with alterations in the substantia nigra pars compacta, dorsal raphe nucleus, basolateral amygdala, and ventral medial prefrontal cortex (Ait Bali et al., 2017). In contrast, the neurogenetic effects of ASD and GLY exposure on the parietal cortex have been less studied. The parietal cortex plays a crucial role in processing varying information, including touch, spatial awareness, and the integration of sensory inputs, consistent with its potential involvement in ASD. First, altered sensory processing is a ubiquitous feature of individuals with autism, including hypersensitivity or hyposensitivity to stimuli (Marco et al., 2011). Second, the parietal cortex is involved in visuospatial processing and skills. Some individuals with autism may have difficulties with spatial tasks and navigation (A. D. Smith, 2015), which could be related to atypical functioning in this brain region. Another aspect to consider is the theory of mind, which pertains to the capacity to comprehend the cognitive aspects of others, encompassing their thoughts, convictions, and motivations. Research has suggested that the parietal cortex may play a role (Mason & Just, 2009); deficits in the theory of mind are commonly observed in individuals with ASD, and disruptions in the parietal cortex could contribute to these difficulties. Last, neuroimaging studies have shown that individuals with ASD often exhibit altered connectivity patterns, including at the parietal cortex level (Xiao et al., 2023). These connectivity abnormalities may underlie some of the cognitive and behavioral characteristics of autism.

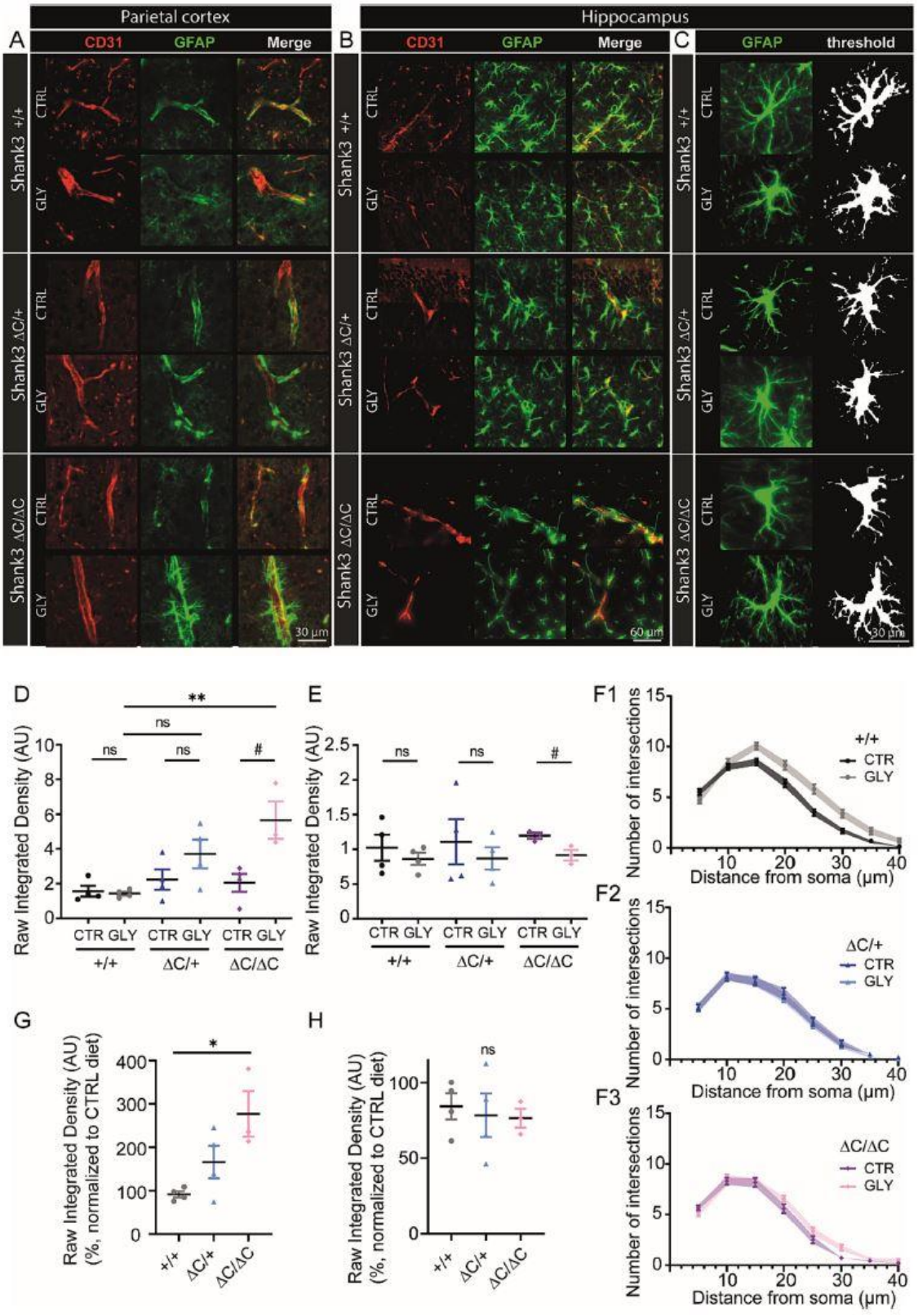

Fig. 5. Perinatal GLY exposure does not induce astrocytes except for cortical perivascular glial reactivity in ΔC/þ mice. Representative images showing GFAP immunofluorescence around vessels stained by CD31 in the parietal cortex (A) and hippocampus **(B). (C)** The morphology of astrocytes (GFAP staining and ImageJ threshold) was assessed using Sholl analysis in the hippocampus of Shank3+/+, Shank3ΔC/+, Shank3ΔC/ΔC treated or not with GLY. **(D, G)** Raw integrated density was measured using ImageJ software around vessels in the parietal cortex (N = 4, ordinary one-way ANOVA, p = 0.0018). It was normalized for each genotype by their

control diet (N = 4, unpaired *t*-test, p = 0.0182). **(E, H)** Raw integrated density was measured using ImageJ software around vessels in the hippocampus (N = 4, ordinary one-way ANOVA, p = 0.7769). It was normalized for each genotype by their control diet (N = 4, ordinary one-way ANOVA, p = 0.8765). **(F1- F3)** Quantification of the Sholl analysis in the hippocampus of Shank3+/+ (F1), Shank3ΔC/+ (F2), Shank3ΔC/ΔC (F3) treated or not with GLY (F, +/+: Two-way ANOVA, p < 0.0001; ΔC/+: Two-way ANOVA, p = 0.4471, ΔC/ΔC: Two-way ANOVA, p = 0.0266). Asterisks indicate statistical significance between genotypes, and hashtags indicate GLY effect (*, #p < 0.05; **, ## p < 0.01; ***, ### p < 0.001; ****, #### p < 0.0001), ns: non-significant.

Fig. 6. Perinatal GLY exposure impairs locomotion and social preference behaviors depending on the presence of Shank3 mutation. (A-C), stereotyped and repetitive behaviors measured by the self-grooming episodes **(D),** locomotion **(E-G-H)**, anxiety **(I)**, memory **(F-J-K)** using the open field apparatus, and social preference using the three chambers test **(L-N)**. Videos were recorded and analyzed through automated video tracking systems (Ethovision, Noldus). **(A-C)** The marble score was evaluated according to the following Score: 0 for a completely buried marble; 1 for a half-buried marble, and 2 for a whole visible marble. +/+ CTR, N = 14; +/+ GLY, N = 12; ΔC/+ CTR, N = 10; ΔC/+ GLY, N = 10; ΔC/ΔC CTR, N = 17; ΔC/ΔC GLY, N = 11. Ordinary one-way ANOVA, p < 0.0001. For each genotype, the marble score was normalized by their control diet. Ordinary one-way ANOVA (p = 0.0300). **(D)** Time spent self-grooming was visually measured during 10 min. +/+ CTR, N = 12; +/+ GLY, N = 11; ΔC/+ CTR, N = 11; ΔC/+ GLY, N = 9; ΔC/ΔC CTR, N = 16; ΔC/ΔC GLY, N = 11. Ordinary one-way ANOVA, p < 0.0001. **(E, G-I)** Total distance traveled and time spent in the center zone were measured over 10 min. +/+ CTR, N = 22; +/+ GLY, N = 10; ΔC/+ CTR, N = 11; ΔC/+ GLY, N = 7; ΔC/ΔC CTR, N = 17; ΔC/ΔC GLY, N = 10. Kruskal- Wallis test (Distance: p = 0.219; time spent in the center zone: p = 0.6140). For each genotype, the distance traveled was normalized by their control diet. Kruskal-Wallis test (p = 0.0030). **(F, J, K)** One hour after the open field, mice were exposed to two similar objects in the open field arena, and one hour later, one familiar object was replaced by a new one. The discrimination ratio was calculated. +/+ CTR, N = 22; +/+ GLY, N = 10; ΔC/+ CTR, N = 11; ΔC/+ GLY, N = 7; ΔC/ΔC CTR, N = 17; ΔC/ΔC GLY, N = 10. Red asterisks: one sample *t*-test (hypothetical mean: 0.5), black asterisks: ordinary one-way ANOVA (p = 0.0011). For each genotype, the discrimination ratio was normalized by their control diet. Ordinary one-way ANOVA (p = 0.0201). **(L-N)** One hour after the habituation period in the empty three-chamber test, an unfamiliar mouse was introduced into one of the empty wire cups and an object into the other. The test mouse was reintroduced, and the time spent sniffing each wire cup was analyzed for 10 min. The social preference ratio was calculated +/+ CTR, N = 10; +/+ GLY, N = 10; ΔC/+ CTR, N = 10; ΔC/+ GLY, N = 8; ΔC/ΔC CTR, N = 8; ΔC/ΔC GLY, N = 10. Red asterisks: one sample *t*-test (hypothetical mean: 0.5), black asterisks: ordinary one-way ANOVA (p < 0.001). The social preference ratio was normalized for each genotype by their control diet. Kruskal-Wallis test (p = 0.0123). Asterisks indicate statistical significance between genotypes, and hashtags indicate GLY effect (*, #p < 0.05; **, ## p < 0.01; ***, ### p < 0.001; ****, #### p < 0.0001), ns: non-significant. (For interpretation of the references to color in this figure legend, the reader is referred to the web version of this article.)

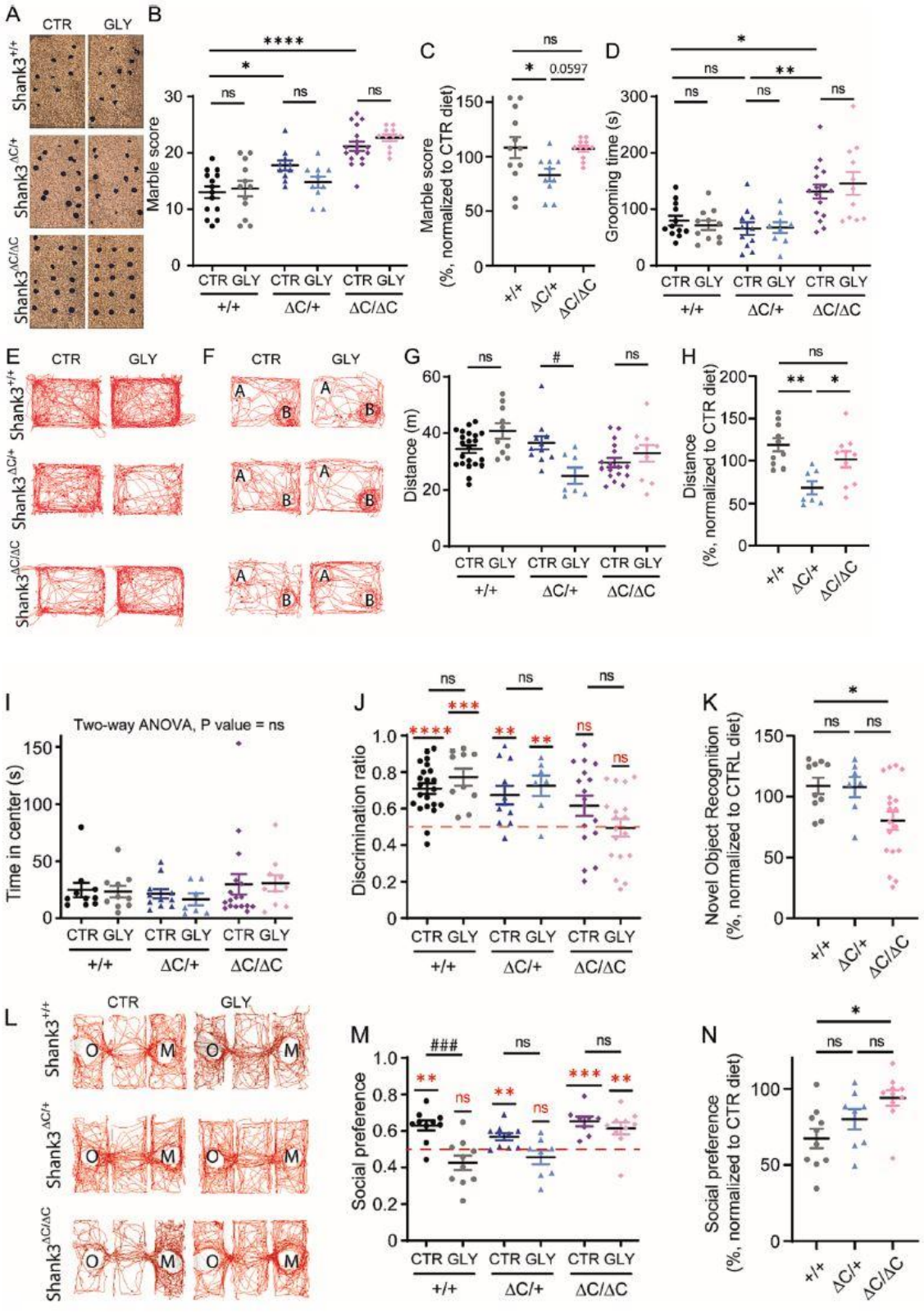

4.2. Morphological biomarkers of neuroinflammatory adaptations

In this experimental setting, we examined the emergence of morphological biomarkers of neuroinflammation in the hippocampus and parietal cortex. The analyses indicate cell adaptations to extra-physiological stimuli, especially in microglial cells. We report an effect

of GLY exposure in cortical microglial cells and perivascular astrocytes. We speculate that, due to spatial heterogeneity (Tan et al., 2020), microglial cells in the somatosensory cortex could be more susceptible to pathological signals. This heterogeneity is particularly relevant to our prenatal-to-post-natal exposure framework because of the differences in developmental glial cell origin, patterns of brain colonization, and gene expression profiles. Delving into the expression patterns of specific pro-and anti-inflammatory cytokines could constitute an independent research topic, primarily due to i) the multifaceted nature of inflammatory equilibriums, ii) the spatiotemporal variability involved, iii) the cellular specificity, iv) the distinction between mRNA and protein levels, which is pivotal given that key cytokines undergo functional activation through post-transcriptional processing. Importantly, GBH was demonstrated to induce brain TNFa expression and to modify the redox balance element experimentally (Ait-Bali et al., 2020; Astiz et al., 2012; El- Shenawy, 2009; Gallegos et al., 2020). A reduced microglial cell ramification and perivascular astrocyte accumulation hint at ongoing cellular reactivity, although these changes are small compared to other brain diseases, such as Alzheimer's disease or multiple sclerosis, where neuroinflammation plays a key role (Hansen et al., 2018; Healy et al., 2022; Klement et al., 2019). Whether glial cells negatively react to NOAEL GLY exposure remains to be confirmed, for instance with in-depth transcriptomic examinations. The latter could reveal whether abnormal neuro-glial interactions exist, a mechanism for the reported behavioral adaptations. Notably, the link between inflammation and ASD is being explored, and studies have provided evidence for a potential causal association (Careaga et al., 2017; Goines & Van De Water, 2010). Immune system abnormalities in individuals with autism might contribute to behavioral impairments (Onore et al., 2012), shaping neural circuits during critical periods of brain development (Bilbo & Schwarz, 2012).

A reduced microglial cell ramification and perivascular astrocyte accumulation hint at ongoing cellular reactivity, although these changes are small compared to other brain diseases, such as Alzheimer's disease or multiple sclerosis, where neuroinflammation plays a key role (Hansen et al., 2018; Healy et al., 2022; Klement et al., 2019). Whether glial cells negatively react to NOAEL GLY exposure remains to be confirmed, for instance with in-depth transcriptomic examinations. The latter could reveal whether abnormal neuro-glial interactions exist, a mechanism for the reported behavioral adaptations. Notably, the link between inflammation and ASD is being explored, and studies have provided evidence for a potential causal association (Careaga et al., 2017; Goines & Van De Water, 2010). Immune system abnormalities in individuals with autism might contribute to behavioral impairments (Onore et al., 2012), shaping neural circuits during critical periods of brain development (Bilbo & Schwarz, 2012).

4.3. Time-dependent effect of GLY exposure: Continuous vs. Postnatal only

We found no substantial impact of GLY exposure when started after weaning, suggesting the deleterious critical importance of the perinatal period. GLY accessibility to the developing

brain and its negative influence on early developmental stages could explain this outcome, although research is needed to explore these possibilities. For instance, during embryonic development, the blood–brain barrier is not fully developed, and the brain is more permeable to various substances. Therefore, the direct action of GLY on the brain would be favored at a developmental age, impacting neuronal wiring and glial activities. Other studies using GLY-based herbicides (GHB) have consistently shown that fetal exposure in rats can cause behavioral alteration in adult offspring, such as depressive-like and anhedonic-like behaviors (Cattani et al., 2017). As discussed in a recent review (Cresto et al., 2023), GLY targets in the brain are still poorly understood. GLY's structural similarity to glutamate and glycine suggests it may directly affect NMDA receptors involved in development, learning, and memory processes. GLY is also a weak inhibitor of acetylcholinesterase; as such, it could cause paralysis (Bridi et al., 2017; Cattani et al., 2017; Gallegos et al., 2020; Larsen et al., 2016), affect dopaminergic neurotransmission (Hernandez-Plata et al., 2015), induce calcium-dependent NMDA-excitotoxicity (Dechartres et al., 2019), cause oxidative stress in the brain (Bali et al., 2019; Cattani et al., 2017), inhibit axonal differentiation (Coullery et al., 2016), lead to motoneuronal damage (Zhang et al., 2017), and affects hippocampal neurogenesis. Alternatively, GLY can indirectly impact brain function by altering the microbiota composition, owing to its inhibitory activity of 5-enolpyruvylshikimate-3-phosphate synthase in plants and bacteria. GLY-induced dysbiosis may affect the central nervous system and contribute to neurological disorders (Del Castilo et al., 2022). At the same time, GLY has been identified to act as an endocrine disruptor, thereby modifying the normal function of the endocrine system during pregnancy, which can lead to sex-different trajectories and disturb embryonic development (Vardakas et al., 2022). Regardless of the mechanisms causing neurological disorders, our study highlights a critical period of vulnerability to GLY exposure.

5. Limitations and conclusions

Our study presents limitations. For instance, we did not directly evaluate the impact of pre-natal NOAEL GLY exposure only. However, our results strongly suggest pregnancy is the critical period for pathological genetic and environmental synergisms. Second, we used NOAEL levels (50 mg/kg bw/day), which could be excessive compared to a realistic scenario. National regulatory agencies indeed report current mean dietary exposure around 0.05 mg/kg bw/day (1% of the European glyphosate-anses-reviews-monitoring-data) or between 0.07 and 0.3 mg/kg bw/day in the US (document EPA-HQ-OPP-2009–0361-0071 EPA). Therefore, our findings should be validated at lower doses, especially regarding the potential impact of prenatal exposure on the developing brain. In contrast, our toxicity study is limited to the effects of GLY, the active agent in commercial GBHs (such as Roundup or RangerPro). However, GBHs contain other ingredients such as polyethylene tallow amine (POEA)-based surfactants, heavy metals, etc., whose acute toxicity is incomparably higher than that of GLY

alone (De Liz Oliveira Cavalli et al., 2013; Mesnage et al., 2013; Nerozzi et al., 2020). From a technical standpoint, we aimed to identify alterations in neuronal activity that have functional significance in vivo, as demonstrated in our behavioral study. While pertinent, investigating post and pre-synaptic termination through histological methods and probably employing high-resolution microscopy exceeds the current capabilities of our research project. Electrophysiological assessments are also needed to identify synaptic-level defects or pinpoint in vivo electrographic rhythm or sleep modifications. Finally, the impact of NOAEL GLY exposure during pregnancy on embryonic survival and development requires further investigation to understand the mechanisms involved, the potential link with postnatal mortality, and the neuroglial phenotypes observed in survivors.

In summary, our results expose the compound effect of environmental contaminants and genetic predispositions on adulthood risk trajectories and frailty. We highlight that if introduced daily and long-term, even NOAEL levels of a specific pollutant could constitute a risk factor for brain adaptations when a synaptic mutation pre-exists.

CRediT authorship contribution statement

SS and NC performed the majority of investigations, methodology, data curation, formal analysis. RC, MJ, EZ and MB participated in data curation and formal analysis. PS, TM, SES and LGP helped with the conceptualization, data curation, methodology, ressources. NM and JP supervised the project, from conceptualisation, funding acquisition, investigation, project administration, validation, to writing the original draft. All authors participated in review and editing.

Declaration of Competing Interest

The authors declare that they have no known competing financial interests or personal relationships that could have appeared to influence the work reported in this paper.

Data availability

No data was used for the research described in the article.

Acknowledgment

This work was supported by EnviroDisorders ANR-16-IDEX-0006 to JP and NM, ANR-Glyphore to LGP, SES, JP, and NM, ANR-Hepatobrain to NM

References

Ait Bali, Y., Ba-Mhamed, S., Bennis, M., 2017. Behavioral and Immunohistochemical Study of the Effects of Subchronic and Chronic Exposure to Glyphosate in Mice. Front. Behav. Neurosci. https://doi.org/10.3389/fnbeh.2017.00146.

Ait-Bali, Y., Ba-M'hamed, S., Gambarotta, G., Sasso`e-Pognetto, M., Giustetto, M., Bennis, M., 2020. Pre- and postnatal exposure to glyphosate-based herbicide causes behavioral and cognitive impairments in adult mice: evidence of cortical ad hippocampal dysfunction. Arch. Toxicol. 94 (5), 1703–1723.

Allen, N.J., Eroglu, C., 2017. Cell Biology of Astrocyte-Synapse Interactions. Neuron 96 (3), 697–708.

Astiz, M., de Alaniz, M.J.T., Marra, C.A., 2012. The oxidative damage and inflammation caused by pesticides are reverted by lipoic acid in rat brain. Neurochem. Int. 61 (7), 1231–1241.

B.M., N., Y., K., L., L., A., M., K.E., S., A., S., C.-F., L., C., S., L.-S., W., V., M., P., P., S., Y., J., M., E.L., C., N.G., C., E.T., G., O., V., C., S., H., L., … J.S., S. (2012). Patterns and rates of exonic de novo mutations in autism spectrum disorders. In *Nature* (Vol. 484, Issue 7397).

Baio, J., Wiggins, L., Christensen, D.L., Maenner, M.J., Daniels, J., Warren, Z., Kurzius-Spencer, M., Zahorodny, W., Robinson, C., Rosenberg, White, T., Durkin, M.S., Imm, P., Nikolaou, L., Yeargin-Allsopp, M., Lee, L.-C., Harrington, R., Lopez, M., Fitzgerald, R.T., Hewitt, A., Pettygrove, S., Constantino, J.N., Vehorn, A., Shenouda, J., Hall-Lande, J., Van, K., Naarden, Braun, Dowling, N.F., 2018. Prevalence of autism spectrum disorder among children aged 8 Years - Autism and developmental disabilities monitoring network, 11 Sites, United States, 2014. MMWR Surveill. Summ. 67 (6), 1–23.

Bali, Y.A., Kaikai, N.-E., Ba-M'hamed, S., Bennis, M., 2019. Learning and memory impairments associated to acetylcholinesterase inhibition and oxidative stress following glyphosate based-herbicide exposure in mice. Toxicology 415, 18–25.

Bilbo, S.D., Schwarz, J.M., 2012. The immune system and developmental programming of brain and behavior. Front. Neuroendocrinol. 33 (3), 267–286. Boeckers, T.M., Bockmann, J.,

Kreutz, M.R., Gundelfinger, E.D., 2002. ProSAP/Shank proteins - A family of higher order organizing molecules of the postsynaptic density with an emerging role in human neurological disease. In *Journal of Neurochemistry* 81 (5), 903–910.

Bonaglia, M.C., Giorda, R., Borgatti, R., Felisari, G., Gagliardi, C., Selicorni, A., Zuffardi, O., 2001. Disruption of the ProSAP2 gene in a t(12;22) (q24.1;q13.3) is associated with the 22q13.3 deletion syndrome. Am. J. Hum. Genet. 69 (2) https:// doi.org/10.1086/321293.

Bourgeron, T., 2015. From the genetic architecture to synaptic plasticity in autism spectrum disorder. In. Nat. Rev. Neurosci. 16 (9), 551–563. https://doi.org/ 10.1038/nrn3992.

Boyd, R.J., Avramopoulos, D., Jantzie, L.L., McCallion, A.S., 2022. Neuroinflammation represents a common theme amongst genetic and environmental risk factors for Alzheimer and Parkinson diseases. In. J. Neuroinflammation 19 (1). https://doi.org/ 10.1186/s12974-022-02584-x.

Bridi, D., Altenhofen, S., Gonzalez, J., Reolon, G., Bonan, C., 2017. Glyphosate and Roundup® alter morphology and behavior in zebrafish. Toxicology 392. https://doi. org/10.1016/j.tox.2017.10.007.

Careaga, M., Rogers, S., Hansen, R.L., Amaral, D.G., Van de Water, J., Ashwood, P., 2017. Immune Endophenotypes in Children With Autism Spectrum Disorder. Biol. Psychiatry 81 (5), 434–441. https://doi.org/10.1016/j.biopsych.2015.08.036.

Cattani, D., de Liz Oliveira Cavalli, V.L., Heinz Rieg, C.E., Domingues, J.T., Dal-Cim, T., Tasca, C.I., Mena Barreto Silva, F.R., Zamoner, A., 2014. Mechanisms underlying the neurotoxicity induced by glyphosate-based herbicide in immature rat hippocampus: Involvement of glutamate excitotoxicity. Toxicology 320, 34–45.

Cattani, D., Cesconetto, P.A., Tavares, M.K., Parisotto, E.B., De Oliveira, P.A., Rieg, C.E. H., Leite, M.C., Prediger, R.D.S., Wendt, N.C., Razzera, G., Filho, D.W., Zamoner, A., 2017. Developmental exposure to glyphosate-based herbicide and depressive-like behavior in adult offspring: Implication of glutamate excitotoxicity and oxidative stress. Toxicology 387, 67–80.

Cattani, D., Struyf, N., Steffensen, V., Bergquist, J., Zamoner, A., Brittebo, E., & Andersson, M. (2021). Perinatal exposure to a glyphosate-based herbicide causes dysregulation of dynorphins and an increase of neural precursor cells in the brain of adult male rats. *Toxicology*, *461*. 10.1016/j.tox.2021.152922.

Costas-Ferreira, C., Dur´an, R., Faro, L.R.F., 2022. Toxic Effects of Glyphosate on the Nervous System: A Systematic Review. In. Int. J. Mol. Sci. 23 (9), 4605. Coullery, R.P., Ferrari, M.E., Rosso, S.B., 2016. Neuronal development and axon growth are altered by glyphosate through a WNT non-canonical signaling pathway. Neurotoxicology 52, 150–161.

Cresto, N., Forner-Piquer, I., Baig, A., Chatterjee, M., Perroy, J., Goracci, J., & Marchi, N. (2023). Pesticides at brain borders: Impact on the blood-brain barrier, neuroinflammation, and neurological risk trajectories. *Chemosphere, 324*. 10.1016/j. chemosphere.2023.138251.

de Araujo, J.S.A., Delgado, I.F., Paumgartten, F.J.R., 2016. Glyphosate and adverse pregnancy outcomes, a systematic review of observational studies. BMC Public Health 16 (1).

de la Paz, M. P., & Canal-Bedia, R. (2021). Autism spectrum disorders in the European Union (ASDEU). In *Siglo Cero* (Vol. 52, Issue 2). 10.14201/SCERO20215224359.

de Liz Oliveira Cavalli, V.L., Cattani, D., Heinz Rieg, C.E., Pierozan, P., Zanatta, L., Benedetti Parisotto, E., Wilhelm Filho, D., Mena Barreto Silva, F.R., Pessoa- Pureur, R., Zamoner, A., 2013. Roundup disrupts male reproductive functions by triggering calcium-mediated cell death in rat testis and Sertoli cells. Free Radic. Biol. Med. 65, 335–346.

Dechartres, J., Pawluski, J.L., Gueguen, M.M., Jablaoui, A., Maguin, E., Rhimi, M., Charlier, T.D., 2019. Glyphosate and glyphosate-based herbicide exposure during the peripartum period affects maternal brain plasticity, maternal behaviour and microbiome. J. Neuroendocrinol. 31 (9) https://doi.org/10.1111/jne.12731.

Del Castilo, I., Neumann, A.S., Lemos, F.S., De Bastiani, M.A., Oliveira, F.L., Zimmer, E. R., Rêgo, A.M., Hardoim, C.C.P., Antunes, L.C.M., Lara, F.A., Figueiredo, C.P., Clarke, J.R., 2022. Lifelong Exposure to a Low-Dose of the Glyphosate-Based Herbicide RoundUp® Causes Intestinal Damage, Gut Dysbiosis, and Behavioral Changes in Mice. Int. J. Mol. Sci. 23 (10) https://doi.org/10.3390/ijms23105583.

Delling, J.P., Boeckers, T.M., 2021. Comparison of SHANK3 deficiency in animal models: phenotypes, treatment strategies, and translational implications. J. Neurodevelopm. Disorders 13 (1). https://doi.org/10.1186/s11689-021-09397-8.

Durand, C.M., Betancur, C., Boeckers, T.M., Bockmann, J., Chaste, P., Fauchereau, F., Nygren, G., Rastam, M., Gillberg, I.C., Anckars¨ater, H., Sponheim, E., Goubran- Botros, H., Delorme, R., Chabane, N., Mouren-Simeoni, M.-C., de Mas, P., Bieth, E., Rog´e, B., H´eron, D., Burglen, L., Gillberg, C., Leboyer, M., Bourgeron, T., 2007. Mutations in the gene encoding the synaptic scaffolding protein SHANK3 are associated with autism spectrum disorders. Nat. Genet. 39 (1), 25–27.

El-Shenawy, N.S., 2009. Oxidative stress responses of rats exposed to Roundup and its active ingredient glyphosate. Environ. Toxicol. Pharmacol. 28 (3), 379–385.

Fagan, J., Bohlen, L., Patton, S., Klein, K., 2020. Organic diet intervention significantly reduces urinary glyphosate levels in U.S. children and adults. Environ. Res. 189 https://doi.org/10.1016/j.envres.2020.109898.

Ferreira, T.A., Blackman, A.V., Oyrer, J., Jayabal, S., Chung, A.J., Watt, A.J., Sj¨ostr¨om, P. J., van Meyel, D.J., 2014. Neuronal morphometry directly from bitmap images. Nat. Methods 11 (10), 982–984.

Gallegos, C.E., Bartos, M., Gumilar, F., Raisman-Vozari, R., Minetti, A., Baier, C.J., 2020. Intranasal glyphosate-based herbicide administration alters the redox balance and the cholinergic system in the mouse brain. Neurotoxicology 77, 205–215.

Gandhi, K., Khan, S., Patrikar, M., Markad, A., Kumar, N., Choudhari, A., Sagar, P., Indurkar, S., 2021. Exposure risk and environmental impacts of glyphosate: Highlights on the toxicity of herbicide co-formulants. Environm. Challenges 4, 100149.

Goines, P., & Van De Water, J. (2010). The immune system's role in the biology of autism. In *Current Opinion in Neurology* (Vol. 23, Issue 2). 10.1097/ WCO.0b013e3283373514.

Hansen, D. V., Hanson, J. E., & Sheng, M. (2018). Microglia in Alzheimer's disease. In *Journal of Cell Biology* (Vol. 217, Issue 2). 10.1083/jcb.201709069.

He, X., Tu, Y., Song, Y., Yang, G., You, M., 2022. The relationship between pesticide exposure during critical neurodevelopment and autism spectrum disorder: A narrative review. Environ. Res. 203, 111902.

Healy, L.M., Stratton, J.A., Kuhlmann, T., Antel, J., 2022. The role of glial cells in multiple sclerosis disease progression. In *Nature Reviews*. Neurology 18 (4), 237–248.

Hernandez-Plata, I., Giordano, M., Díaz-Mu˜noz, M., Rodríguez, V.M., 2015. The herbicide glyphosate causes behavioral changes and alterations in dopaminergic markers in male Sprague-Dawley rat. Neurotoxicology 46, 79–91.

Jaramillo, T.C., Speed, H.E., Xuan, Z., Reimers, J.M., Escamilla, C.O., Weaver, T.P., Liu, S., Filonova, I., Powell, C.M., 2017. Novel Shank3 mutant exhibits behaviors with face validity for autism and altered striatal and hippocampal function. Autism Res. 10 (1), 42–65.

Klement, W., Blaquiere, M., Zub, E., deBock, F., Boux, F., Barbier, E., Audinat, E., Lerner-Natoli, M., Marchi, N., 2019. A pericyte-glia scarring develops at the leaky capillaries in the hippocampus during seizure activity. Epilepsia 60 (7), 1399–1411.

Kouser, M., Speed, H.E., Dewey, C.M., Reimers, J.M., Widman, A.J., Gupta, N., Liu, S., Jaramillo, T.C., Bangash, M., Xiao, B., Worley, P.F., Powell, C.M., 2013. Loss of predominant shank3 isoforms results in hippocampus-dependent impairments in behavior and synaptic transmission. J. Neurosci. 33 (47), 18448–18468. https://doi. org/10.1523/JNEUROSCI.3017-13.2013.

Kozberg, M. G., Yi, I., Freeze, W. M., Auger, C. A., Scherlek, A. A., Greenberg, S. M., & van Veluw, S. J. (2022). Blood-brain barrier leakage and perivascular inflammation in cerebral amyloid angiopathy. *Brain Communications*, *4*(5). 10.1093/braincomms/ fcac245.

Krumm, N., O'Roak, B.J., Shendure, J., Eichler, E.E., 2014. A de novo convergence of autism genetics and molecular neuroscience. Trends Neurosci. 37 (2), 95–105.

Lacroix, R., & Kurrasch, D. M. (2023). Glyphosate toxicity: in vivo, in vitro , and epidemiological evidence . *Toxicological Sciences*. 10.1093/toxsci/kfad018.

Larsen, K.A., Lifschitz, A.L., Lanusse, C.E., Virkel, G.L., 2016. The herbicide glyphosate is a weak inhibitor of acetylcholinesterase in rats. Environmental Toxicology and Pharmacology 45. https://doi.org/10.1016/j.etap.2016.05.012.

Liddelow, S.A., Guttenplan, K.A., Clarke, L.E., Bennett, F.C., Bohlen, C.J., Schirmer, L., Bennett, M.L., Münch, A.E., Chung, W.-S., Peterson, T.C., Wilton, D.K., Frouin, A., Napier, B.A., Panicker, N., Kumar, M., Buckwalter, M.S., Rowitch, D.H., Dawson, V. L., Dawson, T.M., Stevens, B., Barres, B.A., 2017. Neurotoxic reactive astrocytes are induced by activated microglia. Nature 541 (7638), 481–487.

Marco, E.J., Hinkley, L.B.N., Hill, S.S., Nagarajan, S.S., 2011. Sensory processing in autism: A review of neurophysiologic findings. Pediatr. Res. 69 (5 Part 2), 48R–54R.

Martin, J., Taylor, M.J., Lichtenstein, P., 2018. Assessing the evidence for shared genetic risks across psychiatric disorders and traits. Psychol. Med. 48 (11), 1759–1774.

Mason, R.A., Just, M.A., 2009. The role of the theory-of-mind cortical network in the comprehension of narratives. *Linguistics and Language*. Compass 3 (1). https://doi. org/10.1111/j.1749-818X.2008.00122.x.

Mei, Y., Monteiro, P., Zhou, Y., Kim, J.-A., Gao, X., Fu, Z., Feng, G., 2016. Adult restoration of Shank3 expression rescues selective autistic-like phenotypes. Nature 530 (7591), 481–484.

Mesnage, R., Bernay, B., S´eralini, G.-E., 2013. Ethoxylated adjuvants of glyphosate-based herbicides are active principles of human cell toxicity. Toxicology 313 (2-3), 122–128.

Miguel, P.M., Meaney, M.J., Silveira, P.P., 2023. New research perspectives on the interplay between genes and environment on executive functions development. Biol. Psychiatry. https://doi.org/10.1016/j.biopsych.2023.01.008.

Moutin, E., Sakkaki, S., Compan, V., Bouquier, N., Giona, F., Areias, J., Goyet, E., Hemonnot-Girard, A.-L., Seube, V., Benac, N., Chastagnier, Y., Raynaud, F., Audinat, E., Groc, L., Maurice, T., Sala, C., Verpelli, C., Perroy, J., 2020. Restoring Glutamate receptosome dynamics at synapses rescues Autism-like deficits in Shank3- deficient mice. In *In press in Molecular Psychiatry - bioRxiv*. https://doi.org/10.1101/ 2020.12.30.424827.

Moutin, E., Sakkaki, S., Compan, V., Bouquier, N., Giona, F., Areias, J., Goyet, E., Hemonnot-Girard, A.-L., Seube, V., Glasson, B., Benac, N., Chastagnier, Y., Raynaud, F., Audinat, E., Groc, L., Maurice, T., Sala, C., Verpelli, C., Perroy, J., 2021. Restoring glutamate receptosome dynamics at synapses rescues autism-like deficits in Shank3-deficient mice. Mol. Psychiatry 26 (12), 7596–7609.

Nerozzi, C., Recuero, S., Galeati, G., Bucci, D., Spinaci, M., Yeste, M., 2020. Effects of Roundup and its main component, glyphosate, upon mammalian sperm function and survival. Sci. Rep. 10 (1) https://doi.org/10.1038/s41598-020-67538-w.

O ’ Roak, B. J., Vives, L., Girirajan, S., Karakoc, E., Krumm, N., Coe, B. P., Levy, R., Ko, A., Lee, C., Smith, J. D., Turner, E. H., Stanaway, I. B., Vernot, B., Malig, M., Baker, C., Akey, J. M., Borenstein, E., Rieder, M. J., Nickerson, D. A., … Eichler, E. E. (2012). Sporadic autism exomes reveal a highly interconnected protein network of de novo mutations. *Nature*, *485*(7397). 10.1038/nature10989.

Onore, C., Careaga, M., Ashwood, P., 2012. The role of immune dysfunction in the pathophysiology of autism. In *Brain, Behavior, and Immunity*. 26 (3), 383–392.

Peça, J., Feliciano, C., Ting, J.T., Wang, W., Wells, M.F., Venkatraman, T.N., Lascola, C. D., Fu, Z., Feng, G., 2011. Shank3 mutant mice display autistic-like behaviours and striatal dysfunction. Nature 472 (7344), 437–442.

Phelan, K., McDermid, H.E., 2012. The 22q13.3 deletion syndrome (Phelan-McDermid syndrome). Mol. Syndromol. 2 (3–5) https://doi.org/10.1159/000334260.

Ploeger, A., Raijmakers, M. E. J., van der Maas, H. L. J., & Galis, F. (2010). The Association Between Autism and Errors in Early Embryogenesis: What Is the Causal Mechanism? In *Biological Psychiatry* (Vol. 67, Issue 7). 10.1016/j. biopsych.2009.10.010.

Regev, O., Hadar, A., Meiri, G., Flusser, H., Michaelovski, A., Dinstein, I., Hershkovitz, R., & Menashe, I. (2022). Association between ultrasonography foetal anomalies and autism spectrum disorder. Brain : A J. Neurol. 145(12). 10.1093/brain/awac008.

Roberts, J.R., Dawley, E.H., Reigart, J.R., 2019. Children’s low-level pesticide exposure and associations with autism and ADHD: a review. In *Pediatric Res.* 85 (2), 234–241.

Sala, C., Vicidomini, C., Bigi, I., Mossa, A., Verpelli, C., 2015. Shank synaptic scaffold proteins: Keys to understanding the pathogenesis of autism and other synaptic disorders. In. J. Neurochem. 135 (5) https://doi.org/10.1111/jnc.13232.

Sandin, S., Lichtenstein, P., Kuja-Halkola, R., Hultman, C., Larsson, H., Reichenberg, A., 2017. The heritability of autism spectrum disorder. JAMA – J. Am. Med. Assoc. 318 (12), 1182–1184. https://doi.org/10.1001/jama.2017.12141.

Seretopoulos, K., Lamnisos, D., Giannakou, K., 2020. The epidemiology of autism spectrum disorder. In. Arch. Hellenic Med 37 (2).

Shelton, J.F., Hertz-Picciotto, I., Pessah, I.N., 2012. Tipping the balance of autism risk: Potential mechanisms linking pesticides and Autism. In. Environ. Health Perspect. 120 (7), 944–951.

Sheng, M., Kim, E., 2000. The Shank family of scaffold proteins. J Cell Sci . 2000 Jun;113 (Pt 11):1851-6. doi: 10.1242/jcs.113.11.1851.

Smith, L., Klément, W., Dopavogui, L., de Bock, F., Lasserre, F., Barretto, S., Lukowicz, C., Fougerat, A., Polizzi, A., Schaal, B., Patris, B., Denis, C., Feuillet, G., Canlet, C., Jamin, E.L., Debrauwer, L., Mselli-Lakhal, L., Loiseau, N., Guillou, H., Marchi, N., Ellero-Simatos, S., Gamet-Payrastre, L., 2020. Perinatal exposure to a dietary pesticide cocktail does not increase susceptibility to high-fat diet-induced metabolic perturbations at adulthood but modifies urinary and fecal metabolic fingerprints in C57Bl6/J mice. Environ. Int. 144, 106010.

Smith, A. D. (2015). Spatial navigation in autism spectrum disorders: A critical review. In *Frontiers in Psychology* (Vol. 6, Issue JAN). 10.3389/fpsyg.2015.00031.

Sundelin, H.E.K., Stephansson, O., Hultman, C.M., Ludvigsson, J.F., 2018. Pregnancy outcomes in women with autism: A nationwide population-based cohort study. Clin. Epidemiol. 10 https://doi.org/10.2147/CLEP.S176910.

Tan, Y.-L., Yuan, Y.i., Tian, L.i., 2020. Microglial regional heterogeneity and its role in the brain. In. Mol. Psychiatry 25 (2), 351–367.

Taylor, M.J., Martin, J., Lu, Y.i., Brikell, I., Lundstrôm, S., Larsson, H., Lichtenstein, P., 2019. Association of Genetic Risk Factors for Psychiatric Disorders and Traits of These Disorders in a Swedish Population Twin Sample. JAMA Psychiatry 76 (3), 280.

Vardakas, P., Veskoukis, A.S., Rossiou, D., Gournikis, C., Kapetanopoulou, T., Karzi, V., Docea, A.O., Tsatsakis, A., Kouretas, D., 2022. A Mixture of Endocrine Disruptors and the Pesticide Roundup® Induce Oxidative Stress in Rabbit Liver When Administered under the Long-Term Low-Dose Regimen: Reinforcing the Notion of Real-Life Risk Simulation. Toxics 10 (4). https://doi.org/10.3390/toxics10040190.

Vargas, D.L., Nascimbene, C., Krishnan, C., Zimmerman, A.W., Pardo, C.A., 2005. Neuroglial activation and neuroinflammation in the brain of patients with autism. Ann. Neurol. 57 (1), 67–81.

Von Ehrenstein, O.S., Ling, C., Cui, X., Cockburn, M., Park, A.S., Yu, F., Wu, J., Ritz, B., 2019. Prenatal and infant exposure to ambient pesticides and autism spectrum disorder in children: Population based case-control study. The BMJ. https://doi.org/ 10.1136/bmj.l962.

Wang, X., Bey, A.L., Katz, B.M., Badea, A., Kim, N., David, L.K., Duffney, L.J., Kumar, S., Mague, S.D., Hulbert, S.W., Dutta, N., Hayrapetyan, V., Yu, C., Gaidis, E., Zhao, S., Ding, J.-D., Xu, Q., Chung, L., Rodriguiz, R.M., Wang, F., Weinberg, R.J., Wetsel, W. C., Dzirasa, K., Yin, H., Jiang, Y.-H., 2016. Altered mGluR5-Homer scaffolds and corticostriatal connectivity in a Shank3 complete knockout model of autism. Nat. Commun. 7 (1) https://doi.org/10.1038/ncomms11459.

Winstone, J.K., Pathak, K.V., Winslow, W., Piras, I.S., White, J., Sharma, R., Huentelman, M.J., Pirrotte, P., Velazquez, R., 2022. Glyphosate infiltrates the brain and increases pro-

inflammatory cytokine TNFα: implications for neurodegenerative disorders. J. Neuroinflammation 19 (1). https://doi.org/10.1186/s12974-022- 02544-5.

Xiao, Y., Wen, T.H., Kupis, L., Eyler, L.T., Taluja, V., Troxel, J., Goel, D., Lombardo, M.V., Pierce, K., Courchesne, E., 2023. Atypical functional connectivity of temporal cortexwith precuneus and visual regions may be an early-age signature of ASD. Mol. Aut. 14 (1) https://doi.org/10.1186/s13229-023-00543-8.

Zeidan, J., Fombonne, E., Scorah, J., Ibrahim, A., Durkin, M.S., Saxena, S., Yusuf, A., Shih, A., Elsabbagh, M., 2022. Global prevalence of autism: A systematic review update. In *Autism Research* 15 (5), 778–790.

Zhang, S., Xu, J., Kuang, X., Li, S., Li, X., Chen, D., Zhao, X., Feng, X., 2017. Biological impacts of glyphosate on morphology, embryo biomechanics and larval behavior in zebrafish (Danio rerio). Chemosphere 181, 270–280.